

EVALUATION OF THE SERVICE PERFORMANCE OF AN INNOVATIVE PRECAST PRESTRESSED CONCRETE PAVEMENT

A Thesis
presented to
the Faculty of the Graduate School
University of Missouri – Columbia

In Partial Fulfillment
of the Requirements for the Degree
Master of Science

by
GRANT C. LUCKENBILL, E.I.

Dr. Vellore S. Gopalaratnam, P.E., Thesis Advisor

July 2009

The undersigned, appointed by the Dean of the Graduate School, have examined the thesis entitled

**EVALUATION OF THE SERVICE PERFORMANCE OF AN INNOVATIVE
PRECAST PRESTRESSED CONCRETE PAVEMENT**

presented by

Grant C. Luckenbill, E.I.

A candidate for the degree of

Master of Science

and hereby certify that in their opinion it is worthy of acceptance.

Dr. Vellore S. Gopalaratnam, P.E.

Dr. Glenn Washer, P.E.

Dr. Sanjeev K. Khanna

ACKNOWLEDGEMENTS

I would like to extend my gratitude to the Missouri Department of Transportation and Federal Highway Administration for jointly funding the project. Many dedicated individuals from MoDOT and FHWA have demonstrated strong commitments to the advancement of new technologies, specifically John Donahue of MoDOT and Sam Tyson of FHWA. Without their hard work and dedication, pilot projects such as these would not be undertaken. I would like to acknowledge the many professionals at the MoDOT District office in Sikeston, MO who were very supportive of this project. Efforts to accommodate the research team's many requests from Eric Krapf and Michael Chasteen were much appreciated. Jim Copeland took time aside to aid the research team with surveying the pavement. Finally, from MoDOT, I would also like to acknowledge Terry Fields, senior construction inspector, for his help with the research team.

I would also like to commend the work of the Transtec Group including David Merritt, design engineer, for providing design expertise and an extensive background in precast pavements. Additionally I would like to thank the professionals from Concrete Products Incorporated (recently acquired by Prestress Services Industries) and Gaines Construction Company who were very accommodating and aided the research team with coordination efforts during fabrication and construction. Specifically, Andrew Maybee and Jimmy Davis from CPI who were very helpful with the research team during fabrication.

I would like to thank my advisor, Dr. V.S. Gopalaratnam. Dr. Gopal has provided guidance and demanded superior performance during my undergraduate and graduate

degree programs. His unwavering dedication has significantly contributed to my growth as an engineering professional. I will proudly carry the lessons you have taught throughout the rest of my career.

I would also like to thank my parents, family, and friends for aiding in my success. Without their support and guidance, many of these opportunities would not have been made possible.

TABLE OF CONTENTS

| | |
|--|-------------|
| ACKNOWLEDGEMENTS | II |
| TABLE OF CONTENTS | IV |
| LIST OF TABLES | VI |
| LIST OF FIGURES | VII |
| NOMENCLATURE / LIST OF NOTATION | XII |
| ABSTRACT | XIII |
| 1. INTRODUCTION | 1 |
| 1.1. GENERAL INFORMATION AND PROJECT SCOPE..... | 1 |
| 1.1.1. PPCP Project on Interstate 57 and Experimental Investigation..... | 1 |
| 1.1.2. Research Objectives..... | 2 |
| 1.2. OVERVIEW OF PAVEMENT DETAILS AND CONSTRUCTION PRACTICES..... | 3 |
| 1.2.1. Fabrication at the Casting Yard | 4 |
| 1.2.2. Construction of Precast Pavement | 5 |
| 1.2.3. Pavement Panel Designs | 7 |
| 1.3. ORGANIZATION OF THESIS | 11 |
| 2. BACKGROUND INFORMATION | 13 |
| 2.1. OVERVIEW OF PPCP TECHNOLOGY | 13 |
| 2.1.1. Design Considerations for PPCP | 14 |
| 2.2. PPCP PROJECTS IN THE UNITED STATES | 18 |
| 2.2.1. Iowa Approach Slab on Highway 60 | 19 |
| 2.2.2. Interstate 10 in El Monte, CA | 20 |
| 2.2.3. Outer Road near Interstate 35 in Georgetown, TX..... | 20 |
| 2.3. FIELD INSTRUMENTATION OF CONCRETE PROJECTS | 22 |
| 3. EXPERIMENTAL PROGRAM | 25 |
| 3.1. FIELD INSTRUMENTATION..... | 25 |
| 3.1.1. Types of Embedded Instrumentation | 25 |
| 3.1.1.1. Strain-Gage Rebar..... | 25 |
| 3.1.1.2. Vibrating Wire Gage..... | 27 |
| 3.1.1.3. Vibrating Wire Strandmeters | 28 |
| 3.1.1.4. Temperature Gages | 29 |
| 3.1.2. General Design and Placement Considerations | 30 |
| 3.1.3. Instrumentation Layouts | 32 |

| | |
|--|-----------|
| 3.1.4. Data Acquisition System..... | 33 |
| 3.1.5. Remote Monitoring..... | 35 |
| 3.2. LABORATORY EXPERIMENTS | 36 |
| 3.2.1. Materials Testing | 36 |
| 3.2.2. Thermal Investigation of Embedded Instrumentation | 37 |
| 3.3. CHALLENGES FOR REMOTE DATA ACQUISITION | 41 |
| 3.3.1. Excessive Heat Buildup Affecting Sensitive Hardware | 42 |
| 3.3.2. Moisture Intrusion and Corrosion..... | 43 |
| 3.3.3. Lightning Protection | 44 |
| 3.3.4. Snow Removal and Protective Plates | 45 |
| 4. SERVICE PERFORMANCE OF PPCP SYSTEM..... | 47 |
| 4.1. GENERAL INFORMATION..... | 47 |
| 4.2. PAVEMENT THERMAL PERFORMANCE..... | 48 |
| 4.2.1. Temperature Variations | 48 |
| 4.2.2. Daily Thermal Loadings | 49 |
| 4.2.3. Weekly Thermal Behavior..... | 57 |
| 4.2.4. Seasonal Variations in Panel and Global Pavement Responses | 61 |
| 4.3. PAVEMENT RESPONSE DUE TO VEHICULAR LOADING..... | 70 |
| 4.4. EFFECTIVE POST-TENSIONING STRESS DISTRIBUTIONS | 73 |
| 4.4.1. Post-tensioning Stress Distributions affected by Poor Transfer at Joints | 73 |
| 4.4.2. Post-tensioning Stress Losses due to Friction..... | 76 |
| 4.5. TRANSVERSE AND LONGITUDINAL CRACKING..... | 77 |
| 4.5.1. Expert Task Group Meeting in Sikeston, MO | 80 |
| 4.5.2. Visual Crack Surveys..... | 82 |
| 4.6. JOINT PANEL PERFORMANCE..... | 82 |
| 5. CONCLUSIONS | 87 |
| 5.1. PROJECT OBSERVATIONS | 87 |
| 5.2. CONSTRUCTION CHALLENGES | 88 |
| 5.3. SERVICE PERFORMANCE | 89 |
| 5.4. PAVEMENT LONGEVITY | 90 |
| 5.5. RECOMMENDATIONS FOR FUTURE WORK | 90 |
| REFERENCES..... | 92 |
| APPENDIX A | 94 |
| APPENDIX B | 95 |

LIST OF TABLES

| | |
|---|-----------|
| TABLE 4.1 – INSTRUMENT LOCATIONS AND EVENT SUMMARY FOR JOINT PANEL A32 ON JULY 13, 2006..... | 51 |
| TABLE B.1 – LOCATIONS OF INSTRUMENTS USED IN PANEL C1 | 96 |
| TABLE B.2 – LOCATIONS OF INSTRUMENTS USED IN PANEL B1 | 96 |
| TABLE B.3 – LOCATIONS OF INSTRUMENTS USED IN PANEL B2 | 97 |
| TABLE B.4 – LOCATIONS OF INSTRUMENTS USED IN PANEL B3 | 97 |
| TABLE B.5 – LOCATIONS OF INSTRUMENTS USED IN PANEL B4 | 98 |

LIST OF FIGURES

| | |
|---|-----------|
| FIGURE 1.1 – OVERALL PPCP SECTION LAYOUT WITH DRIVING LANES SHOWN (25 PANELS PER SECTION; SECTION 3 IS HEAVILY INSTRUMENTED)..... | 4 |
| FIGURE 1.2 – TYPICAL SECTION OF PPCP PANEL ASSEMBLY AND LAYOUT MODIFIED TO REFLECT MISSOURI PROJECT (MERRITT, McCULLOUGH ET AL. 2000)... | 4 |
| FIGURE 1.3 – JOINT PANEL ON POLYPROPYLENE OVER ASPHALT, AND AGGREGATE BASE (MISSOURI PROJECT) (NOTE: INSTRUMENTATION DATA CABLE EXITING THE END OF THE PANEL)..... | 6 |
| FIGURE 1.4 – PLAN VIEW OF TYPICAL BASE PANEL..... | 8 |
| FIGURE 1.5 – SECTION OF BASE PANEL LOOKING PERPENDICULAR TO TRAFFIC DIRECTION | 8 |
| FIGURE 1.6 – LIFTING ANCHOR, CHAIRS, AND PRESTRESSING STRANDS | 8 |
| FIGURE 1.7 – PLAN VIEW OF TYPICAL JOINT PANEL | 10 |
| FIGURE 1.8 – SECTION OF JOINT PANEL LOOKING PERPENDICULAR TO TRAFFIC..... | 10 |
| FIGURE 1.9 – JOINT PANEL CASTING (LEFT SIDE CURED FOR 1 NIGHT, RIGHT SIDE READY FOR CASTING ON 2ND DAY)..... | 11 |
| FIGURE 2.1 – ILLUSTRATION OF PAVEMENT SECTION SPANNING OVER VOID IN BASE MATERIAL | 15 |
| FIGURE 2.2 – SURFACE FINISHING OF A TYPICAL BASE PANEL AT THE PRECASTING YARD | 16 |
| FIGURE 2.3 – PARTIAL WIDTH PANEL PLACEMENT ON GEORGETOWN FRONTAGE ROAD, TX PPCP (MERRITT 2002)..... | 21 |

| | |
|---|-----------|
| FIGURE 3.1 – SCHEMATIC OF THE STRAIN GAGE CONFIGURATION ON THE STRAIN GAGE REBAR (EATHERTON 1999)..... | 26 |
| FIGURE 3.2 – INSTRUMENTED REBAR SHOWING INSTALLED STRAIN GAGES | 26 |
| FIGURE 3.3 – MODEL 4200 VIBRATING WIRE GAGE FROM GEOKON INCORPORATED.... | 27 |
| FIGURE 3.4 – MODEL 4410 VIBRATING WIRE STRANDMETER, UNSHEATHED | 29 |
| FIGURE 3.5 – THREE THERMOCOUPLES ATTACHED TO A FIBER REBAR COUPLED TO POST-TENSIONING AND PRE-TENSIONING STRANDS..... | 30 |
| FIGURE 3.6 – TYPICAL INSTRUMENTED BASE OR ANCHOR PANEL | 32 |
| FIGURE 3.7 – INSTRUMENTED JOINT PANEL A32 | 32 |
| FIGURE 3.8 – OVERALL VIEW OF TEST-SECTION AND LOCATION OF INSTRUMENTED PANELS (A REFERS TO A JOINT PANEL, B REFERS TO A BASE PANEL, AND C REFERS TO AN ANCHOR PANEL) | 33 |
| FIGURE 3.9 – SIGNAL CABINET WITH MAIN DATA-ACQUISITION EQUIPMENT INSTALLED AT THE EDGE OF RIGHT OF WAY..... | 34 |
| FIGURE 3.10 - JUNCTION BOX INSTALLED IN BLOCKOUT CAST IN OUTSIDE SHOULDER OF PRECAST PAVEMENT PANELS..... | 35 |
| FIGURE 3.11 – UNRESTRAINED INSTRUMENTED REBAR AND VIBRATING WIRE GAGE IN TEMPERATURE CONTROLLED OVEN..... | 38 |
| FIGURE 3.12 – (A) TEMPERATURE HISTORY (B) STRAIN HISTORY OF EMBEDDED AND UNRESTRAINED REBAR INSTRUMENTS | 40 |
| FIGURE 3.13 – IDEALIZATION OF INSTRUMENT RESPONSE DUE TO AN INCREASE IN TEMPERATURE, ΔT | 41 |

| | |
|---|-----------|
| FIGURE 3.14 – SIGNAL CABINET PROTECTED DURING THE HEAT OF THE DAY BY A SHADE ROOF | 43 |
| FIGURE 3.15 – CLOSE-UP OF CJC DAMAGED BY LIGHTNING..... | 45 |
| FIGURE 4.1 – DAY AND NIGHT COOLING TRENDS | 49 |
| FIGURE 4.2 – ONE DAY WINDOW FROM JULY 13, 2006 FOR PANEL A32 (A) TEMPERATURE HISTORY (B) STRAIN HISTORY | 52 |
| FIGURE 4.3 – ONE DAY WINDOW FROM JULY 13, 2006 SHOWING ALL INSTRUMENTS FOR PANEL A32 (A) TEMPERATURE HISTORY (B) STRAIN HISTORY | 54 |
| FIGURE 4.4 – ONE DAY WINDOW FROM JULY 13, 2006 FOR PANEL B3 (A) TEMPERATURE HISTORY (B) STRAIN HISTORY | 55 |
| FIGURE 4.5 – JOINT PANEL A31 DURING MILD TEMPERATURES (LEFT) AND HOT TEMPERATURES (RIGHT)..... | 56 |
| FIGURE 4.6 – MEASURED CONCRETE STRAINS IN PAVEMENT AT A SHORT-TERMED WINDOW (A) TEMPERATURE HISTORY (B) STRAIN HISTORY | 58 |
| FIGURE 4.7 – MEDIUM WINDOW INDICATING WEEKLY HEATING AND DRASTIC COLD FRONT WITH ASSOCIATED CONCRETE STRAINS (A) TEMPERATURE HISTORY (B) STRAIN HISTORY | 60 |
| FIGURE 4.8 – WEEKLY INSTRUMENT HISTORY FOR PANEL B3 (A) TEMPERATURE HISTORY (B) STRAIN HISTORY | 61 |
| FIGURE 4.9 – SIX MONTH WINDOW SHOWING LONGITUDINAL CONCRETE STRAINS IN PANEL B2 AT DIFFERENT LOCATIONS (R2 AND R5) (A) TEMPERATURE HISTORIES (B) STRAIN HISTORIES..... | 63 |

FIGURE 4.10 – SIX MONTH WINDOW SHOWING LONGITUDINAL CONCRETE STRAINS AT IDENTICAL PANEL LOCATION (R2) IN DIFFERENT INSTRUMENTED PANELS (A) TEMPERATURE HISTORIES (B) STRAIN HISTORIES65

FIGURE 4.11 – SIX MONTH WINDOW SHOWING TRANSVERSE CONCRETE STRAINS AT IDENTICAL PANEL LOCATION (R3) IN DIFFERENT INSTRUMENTED PANELS (A) TEMPERATURE HISTORIES (B) STRAIN HISTORIES67

FIGURE 4.12 – TWO MONTH WINDOW SHOWING LONGITUDINAL CONCRETE STRAINS AT IDENTICAL PANEL LOCATION (R1-V1) MEASURED USING INSTRUMENTED REBAR R1 AND VIBRATING WIRE GAGE (V1) (A) TEMPERATURE HISTORY (B) STRAIN HISTORY.....68

FIGURE 4.13 – STRANDMETER RESPONSE AT CENTER OF 250’ TEST SECTION DURING TYPICAL WINTER-TIME TEMPERATURE EXCURSION (A) TEMPERATURE HISTORIES (B) STRAIN HISTORIES.....70

FIGURE 4.14 - TRAFFIC STRAIN (REBAR RESPONSE) IN THE PAVEMENT AT CROWN71

FIGURE 4.15 – DURATION OF TRAFFIC RESPONSE THAT WAS VERIFIED VISUALLY72

FIGURE 4.16 – RESULTING CONCRETE RESPONSE FROM A TRACTOR TRAILER PASSING OVER73

FIGURE 4.17 – CONCRETE STRAIN FOR A TYPICAL BASE PANEL DURING POST-TENSIONING OPERATIONS.....75

FIGURE 4.18 – CONCRETE STRAIN MEASURED AT THE R2 LOCATION (BEGINNING OF OUTSIDE SHOULDER)76

FIGURE 4.19 – AVERAGE POST-TENSIONING CONCRETE STRAIN HISTORIES FOR INSTRUMENTED PANELS77

FIGURE 4.20 - LONGITUDINAL CRACK IN DRIVER SIDE WHEEL LANE.....78

FIGURE 4.21 - SCHEMATIC OF ONE LONGITUDINAL CRACK79

**FIGURE 4.22 – TYPICAL CRACK LOCATIONS OF A 4-PANEL SET OF THE 3RD TEST
SECTION ON MAY 9, 200780**

**FIGURE 4.23 – FLEXIBLE JOINT COMPOUND SQUEEZING OUT ON A HOT DAY WITH
MINOR AMOUNT OF CHIPPING OF RIGID COMPOUND, JOINT PANEL A32
(JUNE 27, 2006).....84**

**FIGURE 4.24 – RIGID JOINT COMPOUND CHIPPED AWAY MORE EXTENSIVELY, JOINT
PANEL A32 (AUGUST 16, 2006).....84**

**FIGURE 4.25 – MODERATE DEGRADATION TO RIGID JOINT COMPOUND, JOINT PANEL
A32 (MAY 9, 2007)85**

**FIGURE A.1 – ONE DAY WINDOW FROM 12/27/2006 FOR PANEL A32 (A) TEMPERATURE
HISTORY (B) STRAIN HISTORY94**

FIGURE B.1 – CONVENTION FOR GAGE LOCATIONS95

NOMENCLATURE / LIST OF NOTATION

| | |
|------------------------------|---|
| T | - TEMPERATURE |
| t | - Time |
| ϵ | - Strain |
| R | - Rebar Strain Reading |
| CTE | - Coefficient of Thermal Expansion |
| PSI | - Pounds per Square Inch |
| A | - Area of Concrete for a Given Cross-Section |
| UPS | - Uninterruptible Power Supply |
| CJC | - Cold Junction Compensation (Circuit) |
| α | - Coefficient of Thermal Expansion |
| BN | - Instrumented Base Panel Label (Number 'N') |
| CN | - Instrumented Anchor Panel Label (Number 'N') |
| A3N | - Instrumented Joint Panel Label (Number 'N') |
| RN | - Instrumented Rebar Label (Number 'N') |
| VN | - Vibrating Wire Gage Label (Number 'N') |
| TN | - Thermocouple Label (Number 'N') |
| N. A. | - Neutral Axis |
| E | - Modulus of Elasticity |
| ν | - Poisson's Ratio |

EVALUATION OF THE SERVICE PERFORMANCE OF AN INNOVATIVE PRECAST PRESTRESSED CONCRETE PAVEMENT

Grant C. Luckenbill, E.I.

Dr. Vellore S. Gopalaratnam, Thesis Advisor

ABSTRACT

Precast Prestressed Concrete Pavement (PPCP) has many advantages over conventional roadway construction techniques. PPCP is the product of an optimization of conventional materials coupled with economical fabrication and transportation means to create a product that exceeds the performance and implementation of current pavement rehabilitation methods. Pre-compressing concrete pavements results in a more efficient, thinner section translating to material savings as well as improved long-term durability. Precast pavement allows faster replacement and rehabilitation of existing roadways as well as providing an economical alternative for new construction to minimize undesirable traffic congestion that causes increased fuel consumption and lost productivity. Decreased construction times are a significant advantage in locations where elevated hazards pose additional risk to worker safety and construction seasons are limited. This project, near Sikeston, MO on Interstate 57, explored feasibility and long-term performance of precast roadway panels subjected to adverse 'Midwest environment'

(extreme temperatures in summer accompanying deicing salts in winter) in addition to evaluation of current construction methods.

The focuses of this thesis are to characterize the thermal behavior and evaluate the overall service performance of the pavement system. Results of thermodynamic experiments, to develop an understanding of the output of strain gage instrumented rebar cast in concrete, are presented. Analysis of results from the investigation include: (a) construction challenges that may affect long term durability (b) local and global prestress distributions within PPCP (c) stress losses during post-tensioning operations (frictional and stress transfer between panels), (d) daily thermal loadings, (e) weekly and seasonal temperature variations and corresponding pavement behavior. Pavement response to traffic loads is presented to contrast daily thermal loadings. Visual crack surveys (longitudinal and transverse) and joint panel performance over the year long evaluation period are discussed.

1. Introduction

1.1. General Information and Project Scope

In conjunction with the Federal Highway Administration, the Missouri Department of Transportation committed to jointly fund and build a new Precast Prestressed Concrete Pavement (PPCP). A section of Interstate 57 near Charleston, MO was chosen for rehabilitation using the PPCP program. The project was completed in December, 2005 and opened to traffic in mid January, 2006. The goal of the Missouri project was to advance technologies developed in recently completed projects in Georgetown, TX and El Monte, CA and evaluate the durability of PPCP in harsh environmental conditions.

1.1.1. PPCP Project on Interstate 57 and Experimental Investigation

The Interstate 57 project was the first large scale PPCP project undertaken in Missouri. Sufficient right of way and funding enabled the installation of asphalt crossovers which aided the construction of the pavement project by relieving time constraints on constructors. In turn, this enabled constructors to experiment and work out the most efficient methods for construction. The site in southern Missouri was also chosen to evaluate the performance of the PPCP technology subjected to harsh environmental conditions. Missouri is known to have extreme seasonal temperature variations. De-icing salts are commonly used on their roadways. The long-term durability of the PPCP test section was “put to the test” with the combination of harsh environmental conditions and heavy truck traffic (approximately 30% of ADT).

1.1.2. Research Objectives

The charge of the University of Missouri – Columbia research team was to evaluate the performance of the PPCP subjected to severe weather and traffic conditions and develop performance data useful for future projects. The team heavily instrumented several panels to quantify pavement performance and validate design assumptions. Due to the broad scope of the research goals of the overall pavement project, this thesis is accompanied by two companion theses by Cody Dailey “Instrumentation and Early Age Performance of an Innovative Prestressed Precast Pavement System” (2006) and Brent Davis “Evaluation of Prestress Losses in an Innovative Prestressed Precast Pavement System” (2006). These reports, which focus on the instrumentation, materials testing, fabrication, early-age behavior, and construction of the PPCP, will be referenced throughout this thesis when overlapping topics are discussed. The project report submitted to MoDOT by the research team, “Performance Evaluation of Precast Prestressed Concrete Pavement, RI03-007,” will also be referenced throughout this paper. This thesis presents thermal and strain gradient data in conjunction with laboratory experiments which focus largely on the characterization of service performance of the PPCP. This data will be helpful in quantifying the effectiveness of PPCP as a rapid rehabilitation pavement alternative to conventional design practice characterized by the following:

- Evaluation of construction methods on the behavior of prestressed system to optimize design and aid in developing preferred practices to expedite construction.

- Study of daily and seasonal temperature dependent effects on the concrete panels and their interaction within the post-tensioned pavement system.
- Overall pavement performance with respect to longevity, durability and how cracking and prestress losses may affect these characteristics.

1.2. Overview of Pavement Details and Construction Practices

The Precast Prestressed Concrete Pavement (PPCP) test section in Missouri replaced a dilapidated 45 year old section of cast-in-place (CIP) concrete just west of Charleston, MO on the northbound lanes of I-57. Three specific types of precast, prestressed panels make up the PPCP system: base panels, joint panels, and anchor panels. They are pre-tensioned in the transverse direction at the casting yard and post-tensioned in the longitudinal direction (parallel to traffic). Each panel is 10'-0" x 38'-0". The 38 ft dimension is perpendicular to traffic. There is a 4'-0" inside shoulder, two 12'-0" driving lanes and a 10'-0" outside shoulder. The panels were cast with a constant 2% grade from the crown to ensure proper drainage.

A 1,010 ft section of conventional cast-in-place pavement was replaced with four sections of post-tensioned precast pavement panels. A typical section consisted of an anchor panel near the middle with eleven or twelve base panels on each side with a joint panel at both ends. These joint panels were heavily reinforced since they contained the post-tensioning blockouts and served to accommodate thermal expansion/contraction of the 250 ft section. Figure 1.1 shows the layout of the four sections of pavement (the highlighted section is heavily instrumented and will be discussed later in detail). Figure 1.2 shows the layout of panels within each individual section.

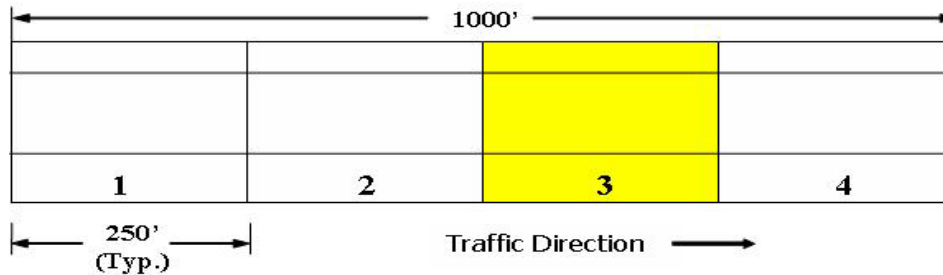


Figure 1.1 – Overall PPCP section layout with driving lanes shown (25 panels per section; Section 3 is heavily instrumented)

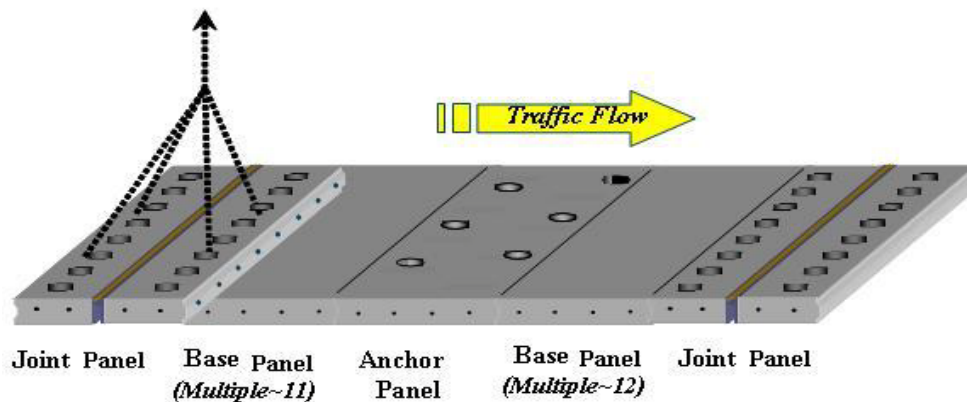


Figure 1.2 – Typical section of PPCP panel assembly and layout modified to reflect Missouri Project (Merritt, McCullough et al. 2000)

1.2.1. Fabrication at the Casting Yard

All 101 precast panels were fabricated by Concrete Products Incorporated (CPI) in Memphis, TN between mid-October and December 2005. They were cast two at a time, crown up, in self-stressing steel casting beds outdoors. The panels were pre-tensioned in the transverse direction using 0.5” uncoated, seven-wire low relaxation strands (270 ksi). The pre-tensioning was incorporated largely to accommodate lifting and transportation stresses. Post-tensioning parallel to the direction of traffic was performed after placement. After casting, the panels were steam cured overnight. This was done to minimize shrinkage and ensure proper curing of the panels. The following

morning, they were de-tensioned and de-molded provided the concrete had reached an initial compressive strength of 3500 psi. Later they were stacked in the storage location of the casting yard to await transportation to the site near Charleston. This single day casting/curing/de-molding of the precast panels enabled the fabricator to turn out two typical base panels per day. The joint panels, which were more complicated in design to fabricate, were cast in two days. An in-depth description of the manufacturing procedures of the precast panels was detailed in (Dailey 2006).

1.2.2. Construction of Precast Pavement

The construction of the PPCP section was performed by Gaines Construction from Wentzville, MO. Typical panel placement rates were between 8 – 25 panels per day. The base, a very critical component of pavement construction, was made up of a 4” asphalt treated base over a 4” permeable crushed stone filter layer. A layer of polypropylene was used as a friction reduction layer and to ease the construction of the pavement. This friction reduction layer is critical in post-tensioned pavement where sub-grade friction reduces the efficiency of prestressing. Figure 1.3 shows an instrumented joint panel on top of the prepared asphalt base with polypropylene sheet clearly visible.

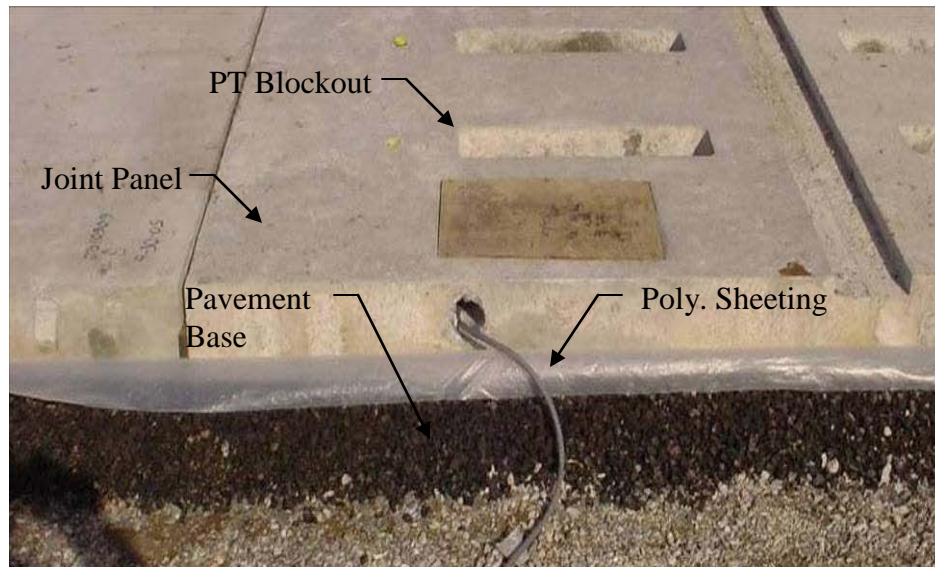


Figure 1.3 – Joint panel on polypropylene over asphalt, and aggregate base (Missouri project) (Note: Instrumentation data cable exiting the end of the panel)

Panels were taken directly from the trucks via crane and positioned at the end of the PPCP section. The joints between the panels were sealed with a slow-curing epoxy, intended to ease placement and seal the joints from water intrusion. Two post-tensioning strands (0.6 inch seven-wire low relaxation strands) were fed through and stressed lightly to recover gaps and slack in the pavement system. However, during complications of feeding post-tensioning strands much of the epoxy placed on the joints was allowed to harden. This resulted in an uneven surface at the joint which impaired uniform load transfer between panels. Additional information regarding the implications of the hardened epoxy layer is discussed in Chapter 4. Wooden and steel shims were placed between panels on the southern edge to aid in recovering pavement misalignment. The usage of rigid shims resulted in uneven distribution of post-tensioning stresses across the panels. Construction challenges such as these were mitigated during construction of the

PPCP pavement. However, adjustments made during construction affected the pre-stressed pavement and complicated the monitored service performance.

1.2.3. Pavement Panel Designs

The Transtec Group from Austin, TX designed the PPCP system consisting of base, anchor, and joint panels. The majority of the panels (92 of 101) were made up of base panels, with 4 anchor and 5 joint panels.

Standard 60 ksi epoxy coated rebar bordered the edges of each base panel and is not shown on the schematics. Its role was to provide typical edge reinforcement to curb cracking and fragmentation of the corners. Each base panel contained eight pre-tensioning strands as shown in Figure 1.4 and Figure 1.5. The pre-tensioning strands located in the top half of the panel were draped to follow the slope of the crown and meet cover requirements at the shoulders. Draping was accomplished by placing varying heights of galvanized chairs under the strands at key locations (see Figure 1.6).

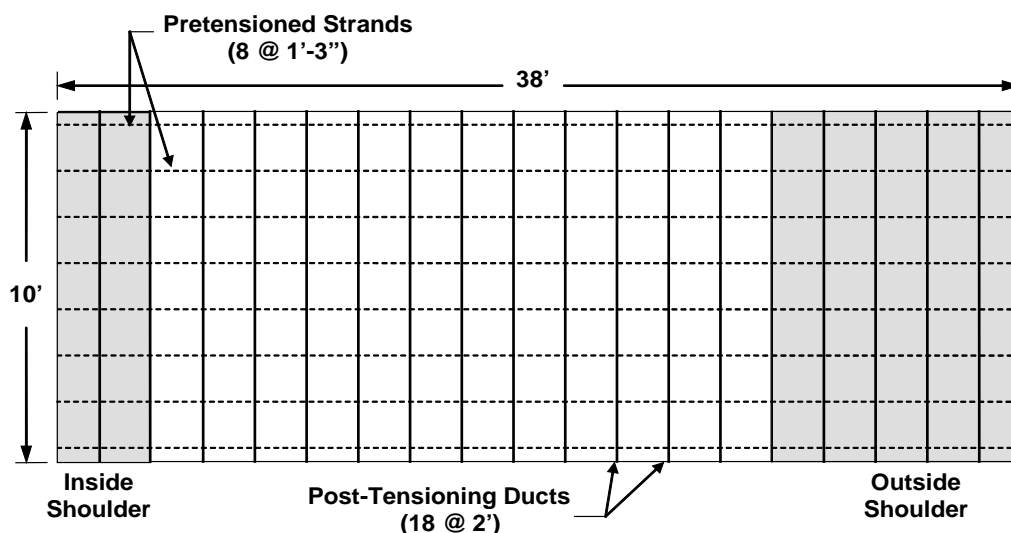


Figure 1.4 – Plan view of typical base panel

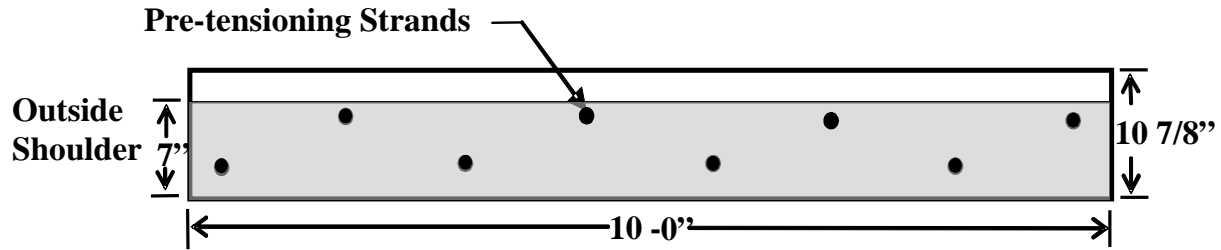


Figure 1.5 – Section of base panel looking perpendicular to traffic direction

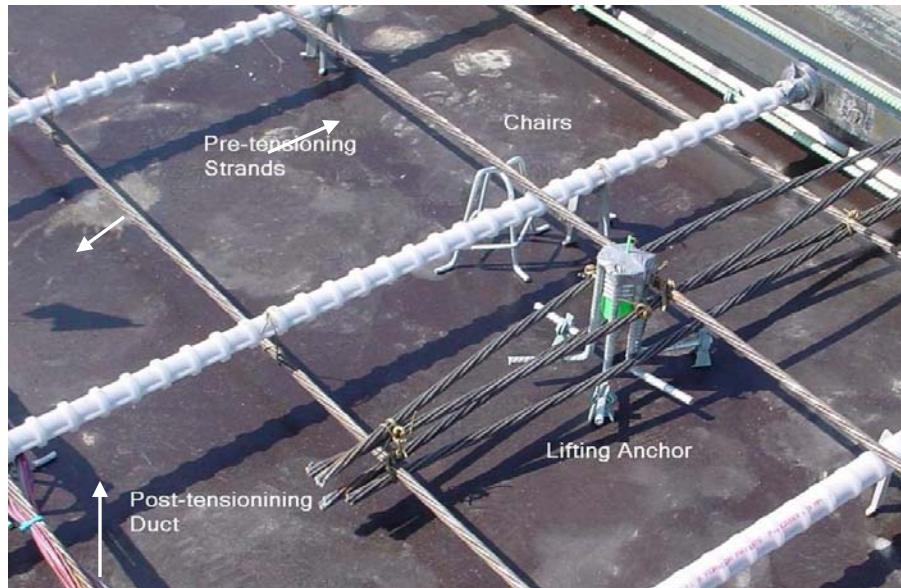


Figure 1.6 –Lifting anchor, chairs, and prestressing strands

Anchor panels are similar to base panels with the addition of full depth holes near the center. These panels are located at the midpoint of each PPCP section and anchor the entire section globally providing a restrained thermal origin to minimize displacements at joints. Reinforcing dowels were driven into the sub grade through the 4 in diameter blocked-out anchor sleeves and grouted. The fabrication of the anchor panels were cast intermittently with the similarly designed base panels.

Joint panel fabrication began mid-December. Due to the complexities of retooling, amount of reinforcement, and functional geometry of the panel, each joint

panel required to be cast in two separate halves. Figure 1.7 shows a plan view of a typical joint panel. Block-outs toward the center of the panel allow access to the post-tensioning ducts, which were filled with grout after post-tensioning. Joint panels have 12 pre-tensioned strands instead of 8 (see Figure 1.8). The top strands are draped with the slope of the crown while the bottom strands are straight. Each half is connected by smooth dowels that provide shear transfer between sections (not shown in schematic). A cold-joint between sections was accomplished by using temporary bulkhead that fastened to the bottom of the bed. The cold-joint was needed to ensure that the joint panel “opened up” during post-tensioning operations. Figure 1.9 shows two halves of a joint panel, one side has cured for one night and the other is ready for casting the following afternoon. Five total joint panels were fabricated for the 1,010 stretch of pavement. The panels at the ends of the PPCP section were cast without post-tensioning block-outs on one half. The side of the panels adjoining to cast-in-place concrete pavement was dowelled in with conventional rebar reinforcement.

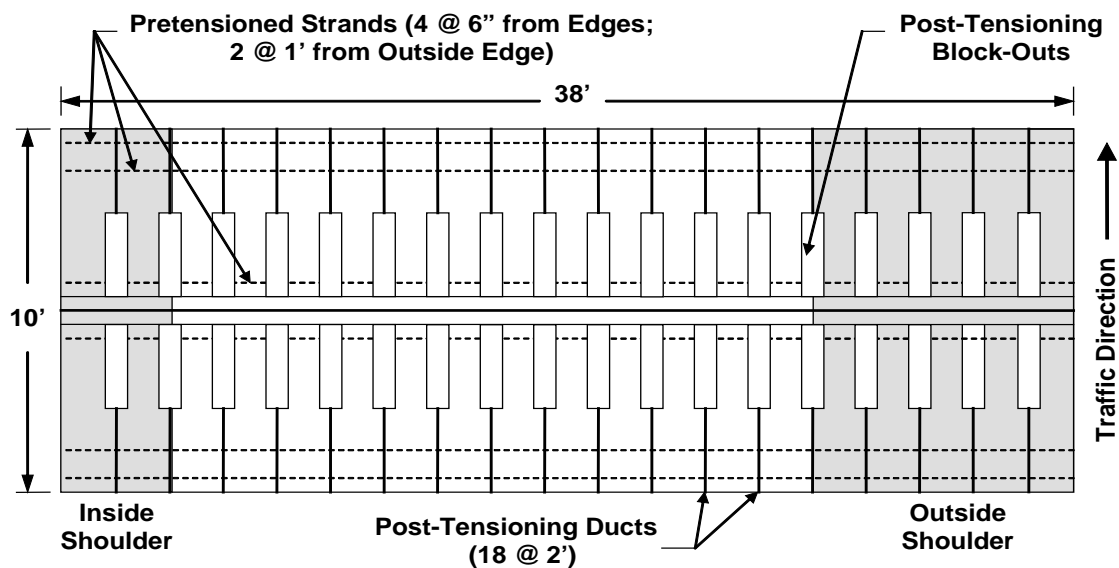


Figure 1.7 – Plan view of typical joint panel

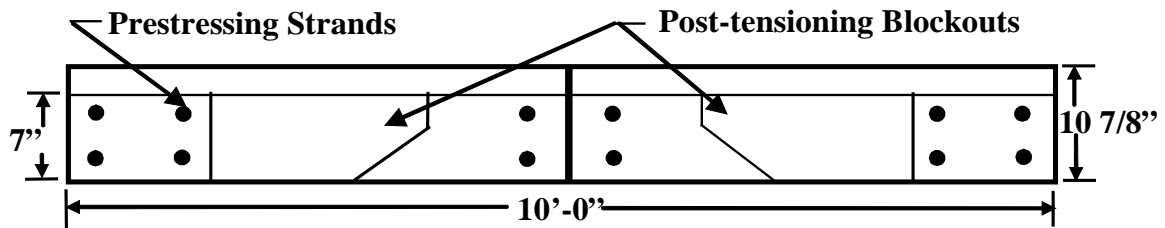


Figure 1.8 – Section of joint panel looking perpendicular to traffic



Figure 1.9 – Joint panel casting (left side cured for 1 night, right side ready for casting on 2nd day)

1.3. Organization of Thesis

Brief overviews of the chapters contained in this thesis are presented in the following paragraphs.

Chapter 1 describes the goals, motivation, and an overview of the design for the Precast Prestressed Concrete Pavement project on I-57.

Chapter 2 provides a literary review of past concrete pavement projects. Discussions on construction designs, prestressed concrete, and instrumentation projects are also presented.

An overview of the experimental program which includes the instrumentation, design and placement, and analyses of the thermal behavior of embedded instrumentation are presented in Chapter 3.

An in-depth look at the service performance of the pavement system is presented in Chapter 4. Thermal and strain gradients are presented for time windows which facilitate discussion on characterization of the factors that affect pavement performance.

This page intentionally left blank.

2. Background Information

2.1. Overview of Precast, Prestressed Concrete Pavement Technology

Precast, Prestressed Concrete Pavement technology is a new approach to pavement design in a field that has seemingly tried all of the possible permutations for optimization of pavement design. PPCP is specifically designed to address some of the problematic areas of conventional cast in place pavement. Current design practices and construction of precast pavement technology have largely been adapted from other applications of prestressed and precast concrete in bridge design. The allure of PPCP technology has benefited from decreased shipping costs and more significant political and monetary benefits from expediting timely pavement projects in high traffic volume areas. Although other prestressed technologies used frequently in bridge deck and girders have proved useful in aiding with the design of PPCP, means of construction and reliability are challenged by clients seeking to employ precast pavement. Pilot PPCP projects have been sought by several DOT's for experimentation to acclimate contractors and evaluate the overall effectiveness as a design alternative to conventional pavement.

The pilot project using PPCP in Missouri was performed to address several issues previous projects have neglected to address. The Missouri Project would evaluate the effectiveness of PPCP as a design alternative in more intimidating climate and subjected to heavy traffic volumes. The previously completed pavement projects have been located in milder climates where the pavement was not subjected to rapid freezing and thawing

and usage of de-icing salts. The performance of PPCP in a harsh environment will serve as a testing platform for further evaluation.

PPCP allows constructors to perform rapid rehabilitation of dilapidated roadways during off peak travel times and place the roadways back into service very rapidly. Traffic congestion due to the presence of construction activities results in, among many other variables, increased fuel consumption and lost work time, or user costs and safety issues related to construction (Merritt 2001). By avoiding peak travel times for construction, safety for workers and travelers is improved by limiting exposure to construction areas. PPCP pavement design alternatives combined with improved safety and timely construction present a clear set of benefits that can be utilized by project managers to decide on the appropriate usage of PPCP. Descriptions of recent PPCP projects are included in the following sections.

2.1.1. Design Considerations for PPCP

PPCP, like many other prestressed concrete applications, utilizes a pre-compressive force to minimize amounts and strength of materials, which results in a more economical design. Constructing an 8” prestressed pavement instead of a 12” conventional pavement results in a savings of over 770 cubic yards of concrete per lane mile. Other advantages are inherent with prestressed systems such as the ability to span voids that develop underneath pavement due to many factors. These voids reduce the support of conventional pavement and create highly stressed localized areas which may reduce the life of the pavement under repetitive wheel loading (See Figure 2.1). Simply

increasing the prestressing force will help the panel act like a thicker pavement (Merritt, McCullough et al. 2000).

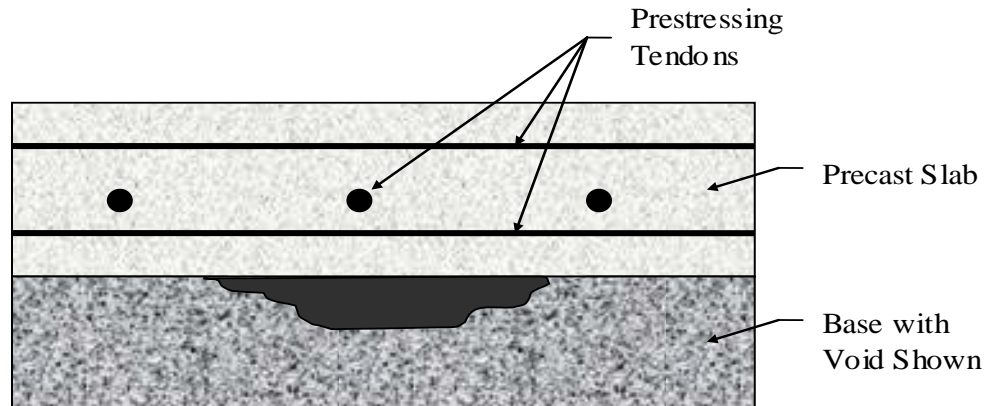


Figure 2.1 – Illustration of pavement section spanning over void in base material

Another inherent benefit from precast pavement is the ability to control the quality of the finished product. Timeliness is held paramount most often when placing conventional pavement due to traffic, workers, and high equipment costs and other constraints. These influences can weigh heavily on builders and can compromise the quality of a finished product. When the pavement is fabricated in advance, more effective quality control, lower tolerances in size and shape, and selective production schedules can be used under controlled conditions since fabricators are not under these constraints (See Figure 2.2).



Figure 2.2 – Surface finishing of a typical base panel at the precasting yard

The controlled environment of a precasting yard also enables a more economical means for controlling the delicate curing process. The panels can be cured in a number of ways to minimize shrinkage effects and residual stresses. Further investigations on casting procedures and curing effects are discussed in (Dailey 2006).

PPCP is very effective in mitigating serviceability problems such as cracking and load transfer. Cracks can spall, fault, and allow water to penetrate the base creating voids under the pavement and facilitate freeze-thaw damage. Crack widths are kept closed by the elastic behavior of the prestressed system. In conventionally reinforced pavement these cracks would open up wider with each successive freeze/thaw cycle and eventually expose the reinforcement and base to water and de-icing salts. This quickly results in degradation of the pavement or creates load-transfer problems meriting repair or replacement. The pre-compression forces in PPCP serve to keep cracks from opening up wide enough to create the aforementioned problems. The shear friction alone, provided

by the pre-compression in a prestressed pavement, provides optimal load transfer across joints and cracks (Merritt, McCullough et al. 2000).

Concrete poured on a base course will tend to have a rough underside, because it takes the shape of the base course, thus increasing the friction of the bottom surface of the pavement. Additionally, concrete poured onto the base will be restrained by a larger mechanical means in which small slivers of concrete are allowed to seep in between the aggregates causing small surface irregularities or “fingers” tying the concrete to the base. When the concrete shrinks during curing, the restraint against the base causes residual stresses in the concrete. These additional stresses are not typically included in design calculations since the geometric constraints are not easily quantified. PPCP has two advantages over CIP concrete since the majority of shrinkage will have occurred at the casting yard and precast panels will have a smooth underside limiting mechanical friction with the base. Fewer shrinkage cracks result in decreased maintenance and repair costs and extend the lifespan of the pavement.

Base preparation is critical to the effectiveness of prestressing and ride quality achieved after installation of PPCP. Polyethylene sheeting has been used to minimize frictional losses between pavement slabs and the base. Not only do slight elevation differences between panels create additional friction by slight miss-alignment of the post-tensioning ducts but can also create an undesirable audible “bump” at panel joints. Diamond grinding at select locations or the application of a smooth leveling course is often required. Shear keys are cast into the joints of the pavement to ensure proper vertical alignment and load transfer.

The performance of PPCP in this and other pilot projects has proven it to be a viable substitute for repair and replacement as well as for new construction of pavement systems. PPCP possesses several design features that make it attractive for implementation on a wide variety of projects such as interchanges, approach slabs, ramps, weigh-in-motion scales, un-bonded overlays, and temporary pavement crossovers. PPCP sections for a 'standard roadway crossover' can be stockpiled and used at multiple locations. Precast pavement panels can also be configured to accommodate unique geometry, typical crowns, cross-slopes and super-elevation transitions. Similar types of unique panel designs and alternative means for pavement system construction methods were well received by precasters and contractors at the Missouri DOT/FHWA showcasing workshop in August of 2006 following the completion of the Missouri Pilot Project.

2.2. PPCP Projects in the United States

The development of PPCP for rapid rehabilitation projects began in the mid 1980's. Projects utilizing CIP prestressed concrete in Texas and South Dakota have proven effective. Since the pavement performed well in these states coupled with advancements in precasting and shipping means facilitated the use of precast slabs. More recently in Georgetown, Texas a frontage road along Interstate 35 was replaced using precast prestressed concrete panels. The experience from the Texas project allowed transportation officials to showcase the benefits of precast construction and demonstrate the advantages of precast panels will serve in urban pavement replacement projects. The following sections describe the recent PPCP projects undertaken throughout the country.

2.2.1. Iowa Approach Slab on Highway 60

A challenging Iowa project successfully incorporated precast prestressed concrete pavement for bridge approach slabs in September 2006. The charge of this project was for Iowa DOT to refine design and construction details of PPCP bridge approach slabs. This project was located on Highway 60 near Sheldon, Iowa. The bridge approach slab tied into a 30 degree skewed, integral abutment for the northbound bridge crossing the Floyd River. The twin southbound bridge was constructed with conventional cast in place approaches to provide a direct comparison in performance during service. The pavement panels were typically 14 ft x 20 ft x 12 inches with panels adjacent to the abutment cast to match the skew. They were assembled in “lane-by-lane” construction on a closed roadway for the new bridge. This project offered a unique bridge approach slab design for IADOT by tying the approach slab into the abutment and moving the expansion joint out to the end of the approach slab. Research by IADOT has shown that removing the expansion joint near the abutment limited water infiltration and erosion of embankment material around the abutment and minimized settlement.

Due to the success of the pilot project, IADOT has scheduled the replacement of failed bridge approach slabs at either end of twin bridges under traffic with PPCP. The end result will be a further understanding and confidence of this pavement system as an alternative means of rehabilitation of bridge approach slabs and replacement of deteriorated or poorly constructed paving notches on high volume roadways and bridges.

2.2.2. I-10 in El Monte, CA

In April 2004 the California Department of Transportation (CalTrans) completed a pilot project using PPCP on Interstate 10 near El Monte, CA. This project involved a little more complexity compared with the Texas project by requiring varying cross-slopes cast into the panels, and nighttime construction operation (Tyson and Merritt 2005). The total length of roadway replaced was 248 ft and consisted of two driving lanes and a 10 ft shoulder that were part of a widening project on I-10. The panels were cast with a flat bottom and a variable depth to maintain a desired cross-slope to match the roadway profile. The pavement was placed on a level 6 inch lean concrete base on top of 8 ½ inch aggregate base. A total of 31 panels were fabricated for the project. The panels were installed at a rate of 15 panels per 3 hours (Transtec 2009). The panels were prestressed transverse to the direction of traffic and post-tensioned in two 124 ft sections longitudinal to traffic (Tyson and Merritt 2005). The pavement widening project was completed successfully and has generated interest for future applications.

2.2.3. Outer road near I-35 in Georgetown, Texas

The first large scale implementation of precast, prestressed pavement was installed on an outer road near I-35 in a jointly funded Texas DOT and FHWA project. The frontage road was located just north of Georgetown, TX. Full and partial width panels were used for this project to test the feasibility of the two panel types. Both types of panels were post-tensioned longitudinally while the partial width panels had additional post-tensioning ducts in the transverse direction (See Figure 2.3). A total of 339 panels were fabricated, of which 123 were full width and 216 were partial width. The full width

panels were wide enough to accommodate two twelve foot lanes an eight foot outside shoulder and a four foot inside shoulder. The partial width panels were 16 feet and 20 feet in width respectively. When placed, the centerline of the roadway matched with the joint between the two panels. The Georgetown pilot project presented many challenges for precast pavement implementation (Merritt 2001). Among the successes were demonstrating that the match-casting is not necessary due to the rugged formwork used in fabrication and geometric mechanisms such as the mating connections cast into each panel that provide for alignment of the post-tensioning ducts in the field. Successful implementation of PPCP technology is dependent on the constructability and flexibility of contractors to develop new practices where standard details have not been developed.



Figure 2.3 – Partial width panel placement on Georgetown Frontage Road, TX PPCP (Merritt 2002)

The pavement in Texas has been in service since March 2002 and no maintenance related issues have been reported (Transtec 2009). Careful planning and willingness to explore innovative means of precast implementation by the DOT, precast supplier, and contractor contributed to the overall success of the project in Georgetown, Texas which opened doors for pilot projects in California and Missouri.

2.3. Field Instrumentation of Concrete Projects

The relatively new age of Precast, Prestressed Concrete Pavement technology compared with that of traditional pavement techniques creates a demand for the demonstration of performance. The caveats that affect the design and performance of various traditional pavement types are well known by designers through experience and testing which dictate the designer's evaluation for pavement design. Field measurement and rigorous evaluation of pilot projects can supply quantifiable information regarding PPCP performance. Strain, temperature, deflection, and durability monitoring are effective means for evaluation and characterization of pavement performance and validation of design. These types of investigations can prove useful for design engineers in the following areas:

- Understanding thermal and frictional response to describe base and sub-base interactions to evaluate proper base materials, thicknesses, loss of support, and usage of bond breakers or friction reducers such as polyethylene sheeting to maximize prestressing efficiency.

- Validate in-service performance of structural design by analyzing strain response of the pavement under traffic loading as well as investigate expected fatigue life and long-term durability.
- Provide an evaluation of stressing operations by monitoring prestressing strands and concrete strain. This data can be used to monitor pavement behavior during and immediately after construction to improve design and construction methods.

This page intentionally left blank.

3. Experimental Program

3.1. Field Instrumentation

The following sections provide an overview of the instrumentation and data acquisition system used for the project. Design, specifications, construction and calibration of custom instrumentation used for the research project are detailed in-depth in (Dailey 2006).

3.1.1. Types of Embedded Instrumentation

Several types of instrumentation were used on this project to quantify and characterize concrete behavior and develop an understanding of the prestressed pavement system at different stages of construction. Direct measurement of concrete strain and prestressed strand strain can be accomplished by embedded strain gages inside of the concrete matrix and attached directly to prestressing strands during casting. The following sections describe the instrumentation used to monitor the performance of PPCP test sections.

3.1.1.1. Strain Gage Rebar

Typical #4, Grade 60 rebar was used to fabricate sensitive strain gage instrumentation for embedment in the concrete pavement panels. Approximately 24 inch long sections were cut and machined smooth in the center to accommodate a temperature-compensating full-bridge circuit. Two gages were installed longitudinally on the rebar and two were installed along the circumference. A schematic of the circuit

used is illustrated in Figure 3.1. The ends of the strain gage rebars were threaded to accommodate gripping for calibration. A completed strain gage rebar is shown in Figure 3.2. Strain gage instrumented rebars are capable of measuring very dynamic events such as stress transfer from strand cutting and traffic loads while in-service. The instruments are also very robust and have a good track record from previous projects completed at the University of Missouri – Columbia.

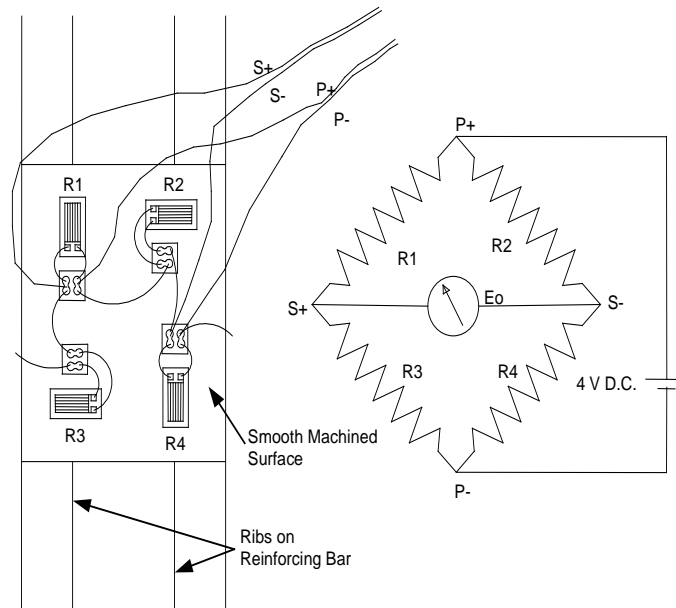


Figure 3.1 – Schematic of the strain gage configuration on the strain gage rebar (Eatherton 1999)



Figure 3.2 – Instrumented Rebar showing installed strain gages

3.1.1.2. Vibrating Wire Gages

Commercially available vibrating wire embedment type strain gages were used to complement the dynamic strain gage instrumented rebar (Model 4200, Geokon Inc.). Vibrating wire gages are reliable for long-term strain measurements due to the nature of its design which does not depend on electrical resistance like a traditional strain gage. The gage consists of a wire stretched between two flanges, an electromagnetic plucking device, and a thermistor used for temperature compensation. The gage operation relies on the change in resonant frequency of the wire based on its length. When one flange displaces relative to the other, the wire is elongated resulting in a change in resonant frequency. This change in resonant frequency can then be related to strain by simple mechanics. The 6 in. gage is depicted in Figure 3.3.

The vibrating wire gages are very useful for long-term strain measurements; however, dynamic events cannot be measured due to settling time of the stretched wire. After embedding the gage in concrete, a zero reading can be taken. At any time the zero reading can be referenced, and the state of strain of the concrete can be determined based on changes in frequency from the base state (zero reading).



Figure 3.3 – Model 4200 vibrating wire gage from Geokon Incorporated

3.1.1.3. Vibrating Wire Strandmeters

Model 4410 Vibrating Wire strandmeters were acquired from Geokon Incorporated for use in the test panels to monitor prestressing strand strain. The gage operates on the same principles as the model 4200 discussed above. However, clamps at either end accommodate fixing to a prestressing strand. All strandmeters were individually calibrated in-house to ensure predictable performance in the field. The gages were encased in a PVC tube filled with grease in order isolate the gage from the surrounding concrete and only measure strain in the post-tensioning strand. Blockouts were cast into the test panels to accommodate the installation of strandmeters prior to stressing, see Figure 3.4.

The strandmeters primary function was to measure the strain of the post-tensioning strands during the stressing operations as well as maintain a record of strand behavior during service. Strand stresses can be correlated with frictional and time-dependent concrete losses to characterize pavement behavior and validate intended design.



Figure 3.4 – Model 4410 vibrating wire Strandmeter, unsheathed

3.1.1.4. Temperature Gages

Type T thermocouples utilizing a copper-constantan connection were used for concrete temperature measurement. The specified temperature range was -328° to 663° F (-200° to 900° C). The thermocouples were cut to length, welded using thermocouple welders, and coated in epoxy at the University of Missouri – Columbia. This type of temperature measuring device is very advantageous due to its robustness, ease of use, and accuracy ($\pm 0.1^{\circ}$ C). Gages were positioned throughout the cross sectional depth, as shown in Figure 3.5, and at various locations across the panel width and length.

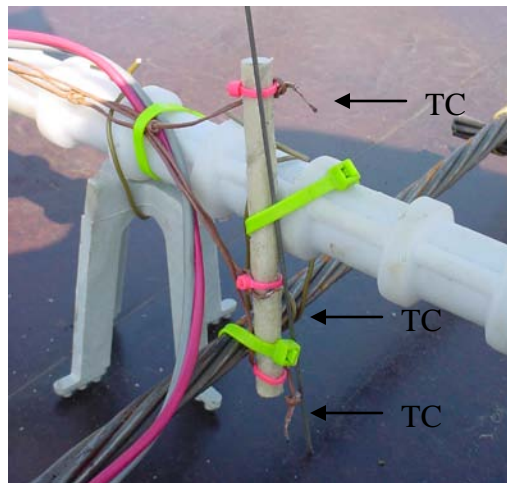


Figure 3.5 – Three thermocouples attached to fiber rebar coupled to post-tensioning and pre-tensioning strands

iButtons manufactured by Dallas Semiconductors were also used to measure temperature (Model DS1922L.) An array of twelve iButtons was used within one of the precast panels as a pilot experiment to validate the welded wire thermocouples and to provide measurement for higher resolution temperature performance through the depth of the pavement. The iButtons store time and temperature logs in self contained memory units and requires only a single lead wire to communicate with a computer or other data

logging device. Lead wires were attached and the entire iButton coated in epoxy to protect from corrosion and grounding inside of the wet concrete.

3.1.2. General Design and Placement Considerations

The precast panels used in the project are identified by two different methods. The identification system used by CPI and Gaines Construction used letters and numbers to signify the different panel types. An “A” panel was a joint panel, a “B” panel was a base panel, and a “C” panel was an anchor panel. Since three different types of joint panels were used, a number after the “A” differentiated the joint panels. Labels “A1” and “A2” represented the joint panels at the north and south limits of the overall pavement test section respectively. The symbol “A3” was used for the three intermediate joint panels in the project.

To differentiate the instrumented panels from the non-instrumented panels the MU research team added a number after the symbols used by the contractors. The panel numbering increased from south to north. For example the four base panels were labeled B1, B2, B3 and B4. The southern-most base panel was B1 and the northern-most was B4. The single instrumented anchor panel was marked C1, and the joint panels were marked A31 and A32 respectively.

The gages within the panels were further identified by their type and location. Vibrating wire gages were marked with a V, instrumented rebar with an R, thermocouples with a T, and strandmeters with an S. The location of the gage was identified by a number after the type of gage. The seven instrumented panels incorporated five different devices to measure strain and temperature of the concrete

along with strain in the post-tensioning strands. Figure 3.6 depicts typical instrumentation in a base or anchor panel and Figure 3.7 shows the instrumentation locations in joint panel A32. Concrete strain was monitored using the strain gage rebars and vibrating wire gages mentioned previously. Post-tensioning strand strain history was measured by vibrating wire strandmeters. Temperature measurements were observed by thermocouples and iButtons (Maxim) embedded in the concrete along with thermistors incorporated inside of the vibrating wire gages.

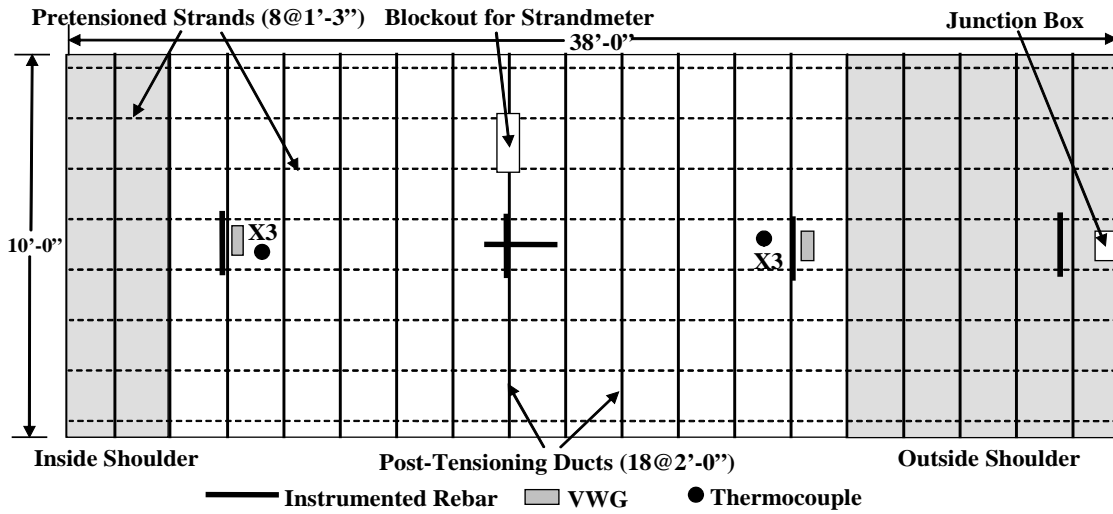


Figure 3.6 – Typical instrumented base or anchor panel

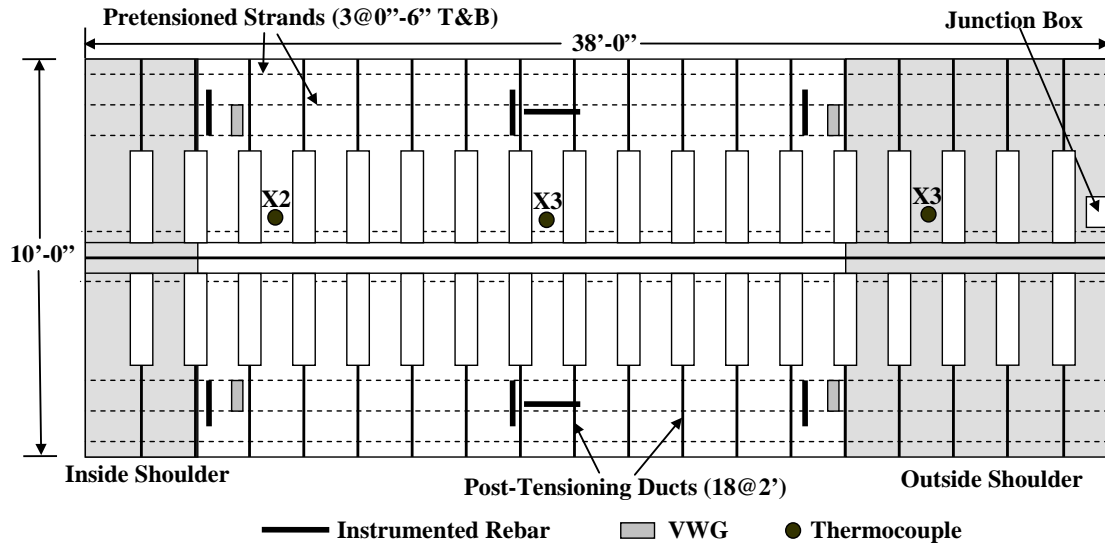


Figure 3.7 – Instrumented joint panel A32

3.1.3. Instrumentation Locations

The pilot project encompassed 1,000 feet of roadway rehabilitation and consisted of four, 250 ft long post-tensioned sections. The primary goal of the research program was evaluate the performance of the PPCP with regard to temperature, loading, local strains, and joint displacements. To accomplish this, the research team decided to focus on a single 250 ft section and instrument panels within this section. Section 3 of the 4 sections along the traffic direction was chosen. It was selected based on its proximity to an AC power source and to limit possible transition effects from conventional concrete pavements adjacent to the PPCP. Four base panels, two joint panels, and one anchor panel were instrumented to characterize the performance of the pavement system under environmental and vehicle loading. Figure 3.8 shows the location of the instrumented panels within the chosen section. The panel marked B4 in Figure 3.8 lies outside the third section and was instrumented for redundancy purposes.

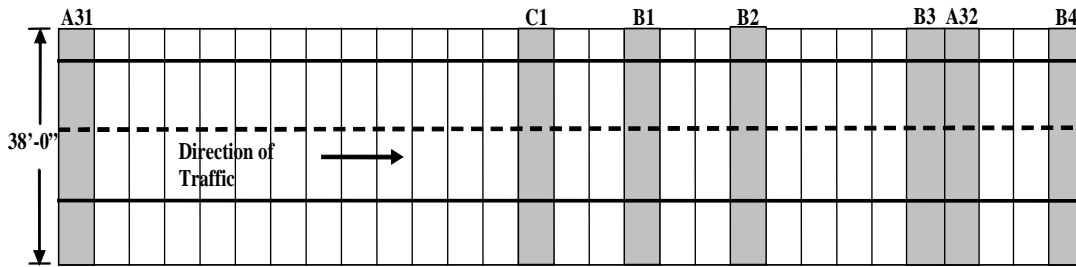


Figure 3.8 – Overall view of test-section and location of instrumented panels (A refers to a joint panel, B refers to a base panel, and C refers to a anchor panel)

3.1.4. Data Acquisition System

A custom data-acquisition system was assembled and used for the monitoring of embedded instrumentation. The data acquisition system consisted of a Campbell Scientific CR10X data logger, (3)-32 differential AM416 relay multiplexers, 110V AC to 12V DC power supply, two AVW1 vibrating wire interfaces, and an NL100 network link interface for remote communication. A centralized location at the test site was chosen to minimize cable lengths and power requirements where the system was housed in an all-weather signal cabinet typically used to house electronics at traffic signals (Figure 3.9).



Figure 3.9 - Signal cabinet with main data-acquisition equipment installed at the edge of right of way

Junction boxes were cast into the shoulder of instrumented panels to provide quick-connect after panel shipment, house a cold-junction compensation circuit needed for thermocouples and voltage regulation circuit for regulating power used by instrumented rebars (Figure 3.10). Voltage regulation at the pavement was necessary due to the voltage loss in the long lengths of cabling to connect instrumentation required due to the large foot print of the project. Multi-pair, stranded wires were run from the junction boxes of each panel back to the data acquisition system for signal transmission.

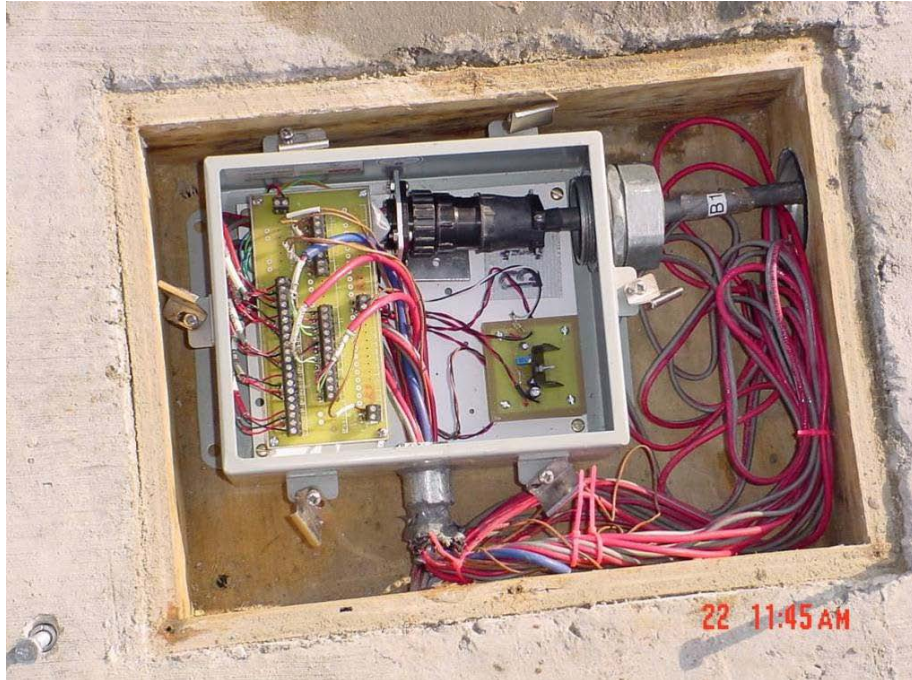


Figure 3.10 - Junction box installed in blockout cast in outside shoulder of precast pavement panels

3.1.5. Remote Monitoring

Proximity to a nearby exit on Interstate-57 where businesses were located enabled the research team to gain access to high speed DSL and electricity. An inexpensive spur line to get closer to the test section was installed by the utility companies for the research team. Luxuries such as electricity and internet service are not commonly available on remote instrumentation sites. Reliable electricity and commercial internet service improved the reliability and simplified powering the data-acquisition systems and instrumentation. Similar long-term monitoring projects performed by the University of Missouri-Columbia located in remote areas required sophisticated, custom power saving circuits accompanying solar panels and back-up generators due to the lack of utilities. These challenges are best avoided if conditions allow and proper planning is allotted during the early phases of site selection.

High-speed DSL enabled the research team to perform real-time data monitoring from the laboratory. Researchers were able to upload customized programs to perform specific tests catered to gather timeline and event specific data on selective instrumentation. Typical programs were designed to perform instrumentation diagnostics, high-frequency readings for wheel load response, monitor prestress levels, and evaluate temperature-strain response during short-term (hours), medium-term (days to weeks), and seasonal weather events. Customizable programs also benefited instrumentation life and electricity savings by utilizing only the gages or thermocouples needed for specific long-term experiments and powering down the remaining instrumentation.

3.2. Laboratory Experiments

3.2.1. Materials Testing

A series of material tests were performed to gain a complete understanding of the composition and behavior of the concrete and materials used in the PPCP system. This data was used to understand pavement behavior resulting from temperature and vehicle loading as well as generate long-term loss models by characterizing shrink, creep, and relaxation to verify results measured in the field. Additionally, samples were prepared to measure the chloride ion resistance which was used to predict pavement durability with respect to salt penetration. Laboratory material testing and results were presented in (Davis 2006).

The following is a summary of the specific tests that were performed.

- Uni-axial Compressive Strength Tests @ 7, 28, and 56 days

- Unrestrained Creep & Shrinkage
- Chloride Permeability Tests
- Freeze Thaw Tests
- Three-Point Flexure Tests

3.2.2. Thermal Investigation of Embedded Instrumentation

Fundamental understanding of how the instrumented rebars behave embedded in a hardened concrete matrix is useful and necessary to analyze results from service measurements.

In an effort to minimize temperature dependent effects, self temperature compensating full bridge circuits were used on the instrumented rebars. In order to understand how the embedded instrumented rebar system responds to thermal and mechanical loads from restraint, laboratory experiments were performed using both unrestrained instrumented rebars as well as instrumented rebars embedded in concrete. One instrumented rebar and one vibrating wire gage were cast into a 6 inch x 6 inch x 24 inch (15.24cm x 15.24cm x 60.96 cm) long concrete specimen in order to duplicate the response of an instrumented rebar embedded in the pavement. Another set of similar instrumentation was supported by metal wires so as to eliminate any restraint to their free movement. Both sets (embedded and unrestrained) of instrumentation were put in an oven and subjected to programmed temperature histories. Figure 3.11 shows the unrestrained instruments suspended by thin wire in the oven.



Figure 3.11 – Unrestrained instrumented rebar and vibrating wire gage in temperature controlled oven

Figure 3.12 shows the responses from the instrumented rebars during the heating of a 14-day old concrete specimen to the temperature history shown in Figure 3.12a. The instantaneous strain (approximately $1 \mu\text{strain}/^\circ\text{C}$) induced in the unrestrained instruments are likely due to temperature dependent non-uniform strain gradients. After several days, the output returned to zero, wherein the rebar had reached a uniform temperature. Elevated temperatures were maintained for nearly 12 days to ensure the entire concrete prism had reached a uniform temperature. The embedded rebar in Figure 3.12 took several days before reaching expected magnitudes of strain based on theoretical predictions of the 52°C temperature excursion. The theoretical rebar strain was calculated by multiplying the change in temperature (ΔT) by the difference in CTE of concrete and steel, which equals $-6.2 \mu\text{strain}/^\circ\text{C}$. The embedded rebar strain was compressive in nature with an increase in temperature, which supports the logic used to describe the embedded instrumentation performance. The magnitude of strain in the embedded rebar reached higher values than computed from ΔT . This larger magnitude is attributed to drying shrinkage, which was exaggerated by desiccation due to the high

temperatures in the oven (for a relatively green concrete, 14 days old when experimented was started). This was confirmed after the heat had been turned off. The resulting magnitude of residual strain measured by the embedded rebar was equal to the difference between the theoretical embedded rebar strain and actual embedded rebar strain (approximately 100 μ strain of drying shrinkage strain). Concrete strain was calculated by multiplying the scalar $(-6 / 6.2)$, which was calculated from the difference in CTE's of concrete and the rebar. It can be seen in Figure 3.12 that after 11 days, the temperature measured by the thermocouple (wrapped up with the embedded rebar, R17), had reached room temperature rather quickly yet there was still strain recovery over the following days that mimicked the unrestrained rebar signal.

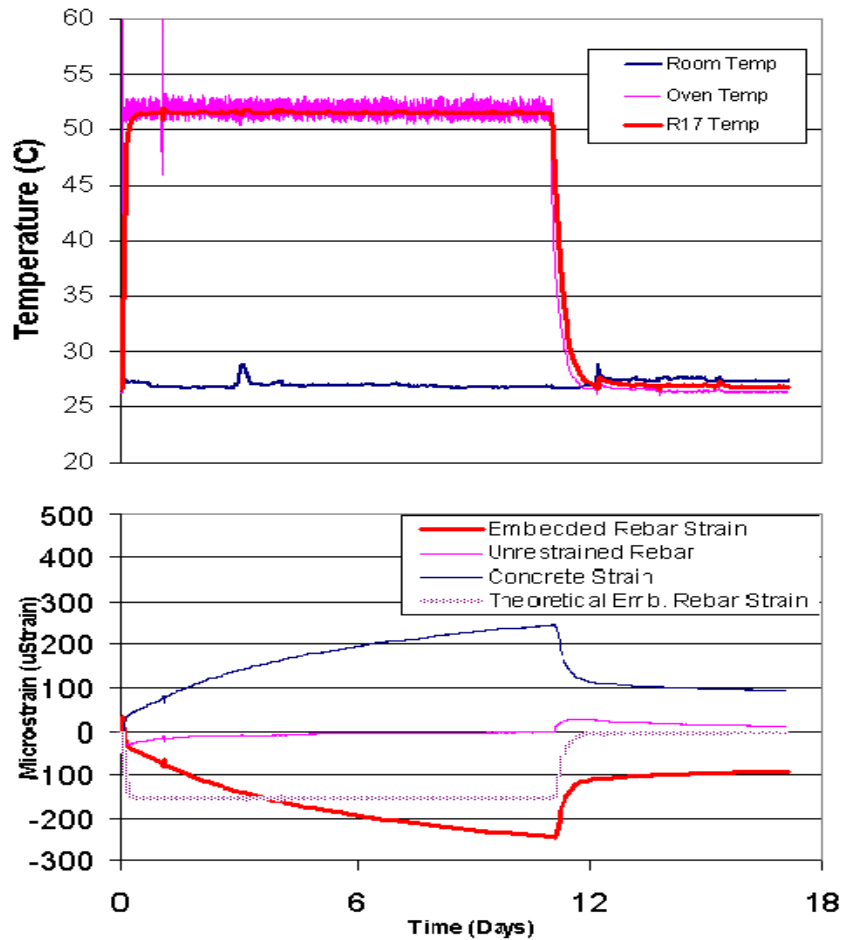
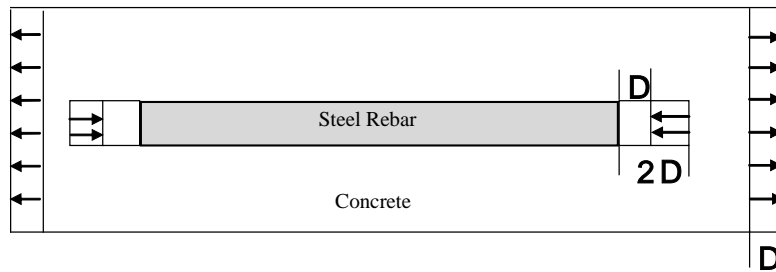


Figure 3.12 – (a) Temperature history (b) Strain history of embedded and unrestrained rebar instruments

The concrete strain measurements during service are largely dictated by thermal excursions from everyday heating and cooling. These analyses have led to the following idealization and subsequent equation that was used to interpret the service performance data of the instrumented panel sections.

- The concrete ($6 \mu\text{strain}/^\circ\text{C}$) has a CTE of roughly half that of the embedded steel ($12.2 \mu\text{strain}/^\circ\text{C}$) instrument.
- The system experiences a $+\Delta T$
- The concrete expands Δ , and the steel wants to expand 2Δ . Yet the steel is restrained by the concrete to only Δ .

- Hence, the strain in the instrumented rebar is measured as a compressive Δ to a heating of the system.



$$\Delta \varepsilon_{Concrete} = \left(\frac{CTE_{concrete}}{CTE_{concrete} - CTE_{rebar}} \right) \times (R_1 - R_0)$$

Figure 3.13 – Idealization of instrument response due to an increase in temperature, ΔT

3.3. Challenges for Remote Data-Acquisition

Many challenges had to be addressed with respect to the service performance of the instrumentation and data acquisition system developed for the precast project. These challenges sometimes resulted in delays because of the need to undertake several repair visits after severe weather-related events. In spite of more than adequate planning and installation of safety systems, such extensive instrumentation with a network of electrical conductors spanning over 9,000 square feet serves as an easy sink for electrical activity during thunder storms. A summary of the various challenges and appropriate remedies to mitigate each problem are listed here so as to be helpful for future projects of a similar nature.

3.3.1. Excessive Heat Build-up affecting Sensitive Hardware

The signal cabinet that housed the power supply, communications and data acquisition system was located in a field just beyond the shoulder alongside the instrumented pavement section. This box was exposed to fairly high ambient temperatures (build-up of temperature in excess of 160°F during peak summer days was measured). These excessive ambient temperatures and resistive heat build up in the voltage regulators resulted in malfunctioning of the voltage regulation circuitry that supplied DC power to the instrumented rebars. A “belt-and-suspenders” approach helped alleviate this problem. First a roof was built to protect the signal box from direct sun exposure (Figure 3.14). Secondly, two heavy-duty equipment fans were installed in the signal cabinet that were on at all times and allowed flow of air through the cabinet. Third, all the voltage regulators were replaced with military grade regulators that were specified for higher operating temperatures. And fourth, all the regulators (those in the signal cabinet as well as the individual panel terminal boxes) were provided with larger aluminum heat dissipation fins. Collectively all of these four upgrades essentially eliminated problems associated with excessive heat build-up and associated electronic instabilities.



Figure 3.14 – Signal cabinet protected during the heat of the day by a shade roof

3.3.2. Moisture Intrusion and Corrosion

For an instrumentation project such as this, it is necessary to build-in sufficient moisture protection for the electronic components and associated circuitry. While the terminal boxes embedded in each of the instrumented panels were specified to be hermetically sealed, the holes that allowed instrumentation cables into the box, also allowed moist air even while the holes were sealed with silicone. The circuit boards were also mounted with sufficient clearance from the bottom of the terminal boxes using spacer legs to avoid standing water from interfering with their intended operations. The circuit boards were additionally sprayed with a non-conducting urethane spray to waterproof them. The terminal boxes also contained desiccants in cloth bags. With adverse weather, a significant amount of precipitation and infiltration of moist air, the electronics in the terminal boxes were exposed to moisture and on rare occasions (in some panels) a small amount of standing water (inside the terminal boxes). On a few occasions the moisture shorted the printed circuit boards in these terminal boxes despite all the protective actions and had to be repaired or replaced. Continued monitoring of these

terminal boxes during inspection visits, cleaning, caulking and replacement of desiccant bags helped mitigate the moisture problem.

3.3.3. Lightning Protection

Even while all cables were well shielded and grounded, lightning strikes tripped the protective circuit breakers, damaged the uninterruptible power supply (UPS), several voltage regulators and cold junction compensation (CJC) circuitry. While studying the “as-implemented” circuitry to fix the problem, it came to light that while the circuit was well protected against a lightning strike on the power pole side of the system, there was little protection against voltage surges on the instrumentation side of the circuitry. Close-up of a CJC circuit board damaged by a lightning strike is shown in Figure 3.15. Diodes, which prevent the reverse flow of electricity, were employed in all of the instrumentation lines and across all of the voltage regulators to ensure that any electrical surge would be discharged to the earth ground. After observing that the most viable method to properly ground the system for lightning affected the magnitudes of the outputs from the instruments due to a ground loop differential, a spark gap was employed to prevent adversely affecting the system during normal operating conditions and still provide lightning protection when needed.

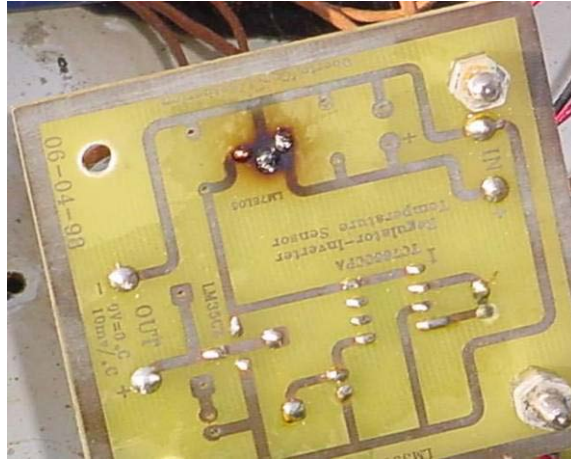


Figure 3.15 – Close-up of CJC damaged by lightning

3.3.4. Snow Removal and Protective Plates

During the first winter (January 2006), snow plows sheared off the bolts securing the protective covers of the terminal boxes that were slightly above the surface of the pavement. This allowed water to get in to the terminal boxes. Use of thinner (but yet sturdy to withstand traffic loads) protective cover plates with counter-sunk recesses allowed enough clearance so that the bolt heads could be flush with the top surface of the protective plates. This mechanical upgrade ensured that no repeat of such damage occurred during the second winter (January 2007).

This page intentionally left blank.

4. Service Performance of PPCP System

4.1. General Information

A summary of service performance results from the year long monitoring of the instrumented pavement panels is presented in this chapter. Typical daily, short-term (few days) and longer term seasonal temperature and strain excursions are presented and discussed. Vehicular loading events were measured and are presented. An evaluation of the causes and characterization of prestress losses are presented and discussed. Also included are observations for visual inspections carried out during the regular field inspections of the pavement test sections. Since the more consistent data from the instrumented rebars were available for the majority of the project duration, they are used primarily for figures and discussions. The vibrating wire data, when available, had been used to confirm magnitudes of strain excursions measured using the instrumented rebars. However plots for vibrating wire strain data which are typically noisy and intermittent due to frequent malfunctions and over-range chipping are not included. As a consequence these results are not presented in this chapter.

It should be noted that strain data presented here includes the combined effects of thermal loading, vehicular loading, viscous loading due to creep, shrinkage and relaxation, and loads due to sub grade movement. However, given the time windows of interest and sample rates of data acquisition, the dominant influence is due to thermal loading. The effect of vehicular loading is isolated in one plot where a significantly higher data acquisition rate was intentionally used to highlight this effect.

Strain measurements were recorded using instrumented rebars and vibrating wire gages. Due to adverse weather events, 5 of 12 vibrating wire gages were damaged during the storms of spring 2006 and operated intermittently. The remaining vibrating wire gages have operated consistently throughout the duration of the project. More details on the challenges faced with the data acquisition system can be found in Section 3.3. It should be kept in mind that electrical drift can affect long term measurements using resistance type strain gages. Careful planning and design of the instruments and data acquisition system kept electrical complications at a minimum compared to true strain signal output. Daily outputs of strain gages were also subject to voltage fluctuations caused by temperature changes and were adjusted.

In looking at the strain histories generally presented in this thesis it is important to recognize that the zero strain reference at the start of each plot doesn't represent actual "zero strain" value but is a reference for incremental excursions shown. In other words, negative strains do not necessarily mean compression but are merely less tension. This is typical for strain-gage based transducers where "zeroing" long term measurements to study incremental events is more important than studying actual strain magnitudes.

4.2. Pavement Thermal Behavior

4.2.1. Temperature Variations

Thermal loads constitute the single most important influence on pavement strains observed on a daily basis. However, since the pavement does not have a uniform cross-section, heating, heat-retention and cooling occur at different rates for different cross-sections resulting in gradient effects. Proximity within the concrete matrix to both air

and ground work as heat sources and sinks. This enables the thinner sections to heat and cool more quickly than the thicker section around the crown. Figure 4.1 highlights the potential for differential heating and cooling using a typical summer day and night. Point A on the pavement panel is at the outer edge of the thinner section, and during the daytime it heats quicker than the rest of the panel that is exposed to the air due to the thicker cross section and proximity to exposed surfaces. Point B is the last portion of the concrete section to heat up during the day, and during the night is the last section to cool down (Point C). Similar trends in reverse are anticipated during cooling cycles during nights or winter related seasonal cold fronts.

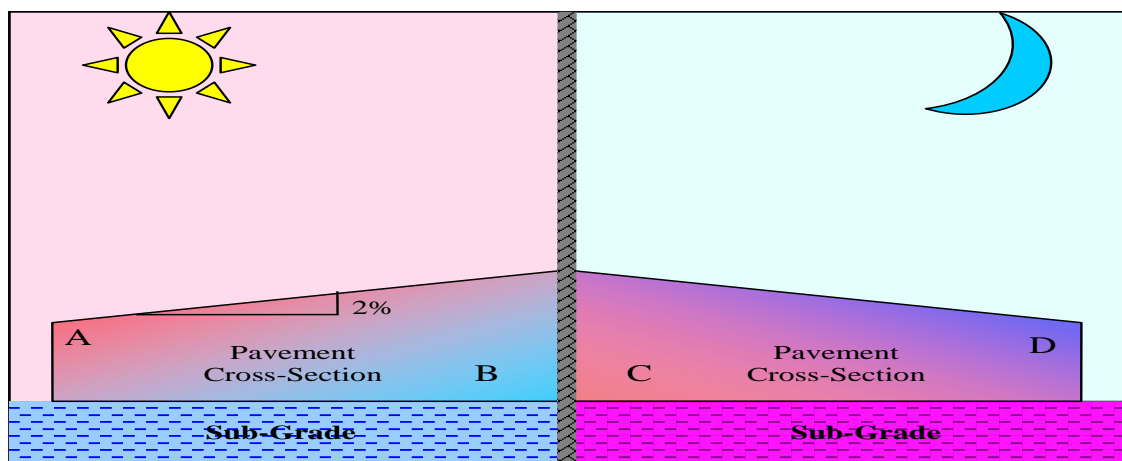


Figure 4.1 – Day and Night Cooling Trends

4.2.2. Daily Thermal Loadings

Pavement response, calculated from individual instruments, have a thermal component plus effects of restraint due to sub-grade movements, thermal gradients, and eccentric prestressing.

The magnitude of recorded concrete temperature and rate of thermal loading is affected by proximity of the particular section to exposed surfaces and thickness at that location. Figure 4.2b indicates the daily concrete response at three instrumented rebar locations (R1, R3 and R4 see inset) that are parallel to the traffic direction. Temperatures recorded close to the strain measurement locations are reported in Figure 4.2a.

Theoretical concrete strain history was predicted by averaging the three temperature change measurements and multiplying by the CTE of concrete assumed to be $6 \mu\text{strain}/^\circ\text{C}$. The locations of the instruments and thicknesses of corresponding pavement are shown in Table 4.1 (depth of instrument from driving surface). The magnitudes of the recorded temperatures are reflective of both the thicknesses of the pavement and proximity to the nearest exposed surface. A32_V3t at R7 is closer to two surfaces than R1 or R3. This may explain why the temperature excursion at R7 is the highest. Higher temperature swings produced larger strain excursions, even at localized panel locations. R7 has a ΔT of 14.4°C but exhibits a strain differential of $107 \mu\text{strain}$. If the response were attributed only to the temperature change, R7 would only indicate $86.5 \mu\text{strain}$. The difference between the expected thermal strain and the observed strain excursion is $20.5 \mu\text{strain}$ and is consistent with the strain excursions of R1 and R3 shown in Figure 4.2. This difference can be attributed to the several additional constraints described earlier.

Table 4.1 – Instrument Locations and Event Summary for Joint Panel A32 on July 13, 2006

| Instrument | Pavement Thickness (inches) | Instrument Depth (inches) | Temperature Change (celsius) | Daily Strain Excursion (μ strain) |
|------------|--------------------------------|------------------------------|---------------------------------|---|
| Rebar 1 | 8.2 | 4.2 | 8.8 | 83 |
| Rebar 3 | 10.9 | 5.5 | 10.4 | 82 |
| Rebar 7 | 9.3 | 4.8 | 14.4 | 107 |

The duration that the strain level is sustained at peak levels during temperature extremes is correlated well with pavement thickness at the location. In Figure 4.2 , R1 peaks at 5 hours and starts to indicate less tension faster than R3 and R7. R3 and R7 exhibit similar thickness dependent strain response.

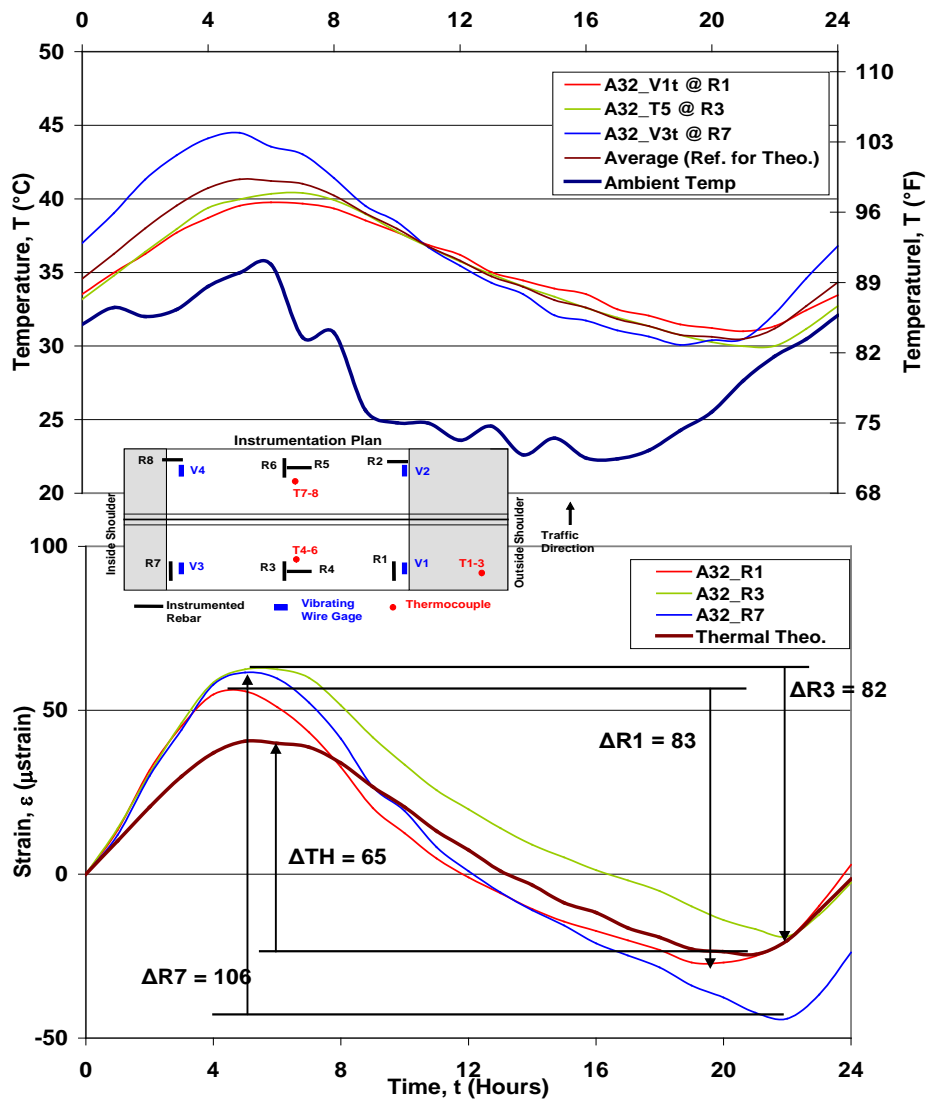


Figure 4.2 – One day window from July 13, 2006 for Panel A32 (a) temperature history (b) strain history

The relative strain response from longitudinal and transverse concrete strains was also studied in relation to the daily thermal history. Figure 4.3a and Figure 4.3b shows the response from instrumented rebars during a 24-hour window for a typical summer day. Strains proportional to the local temperatures of 35 to 60 μstrain can be observed for the rebars aligned along the traffic direction (longitudinal rebars R1, R3, and R7). R5

which is located transverse to traffic indicates much larger tensile strains on the order of 90 μ strain. The tensile strains of R5 in Figure 4.3b are also sustained at the high magnitudes of strain for much longer than peak strains sustained by the longitudinal rebars. The higher tensile strains and durations are also illustrated for the transverse rebar, R3 in panel B3 (Figure 4.4b). Similar responses for the transverse strain behavior were recorded for a typical winter day and presented in Appendix A (See Figure A.1), highlighting the fact that this behavior is not unique to significantly different average ambient temperatures (30°C for the summer day shown versus 8°C for the winter day).

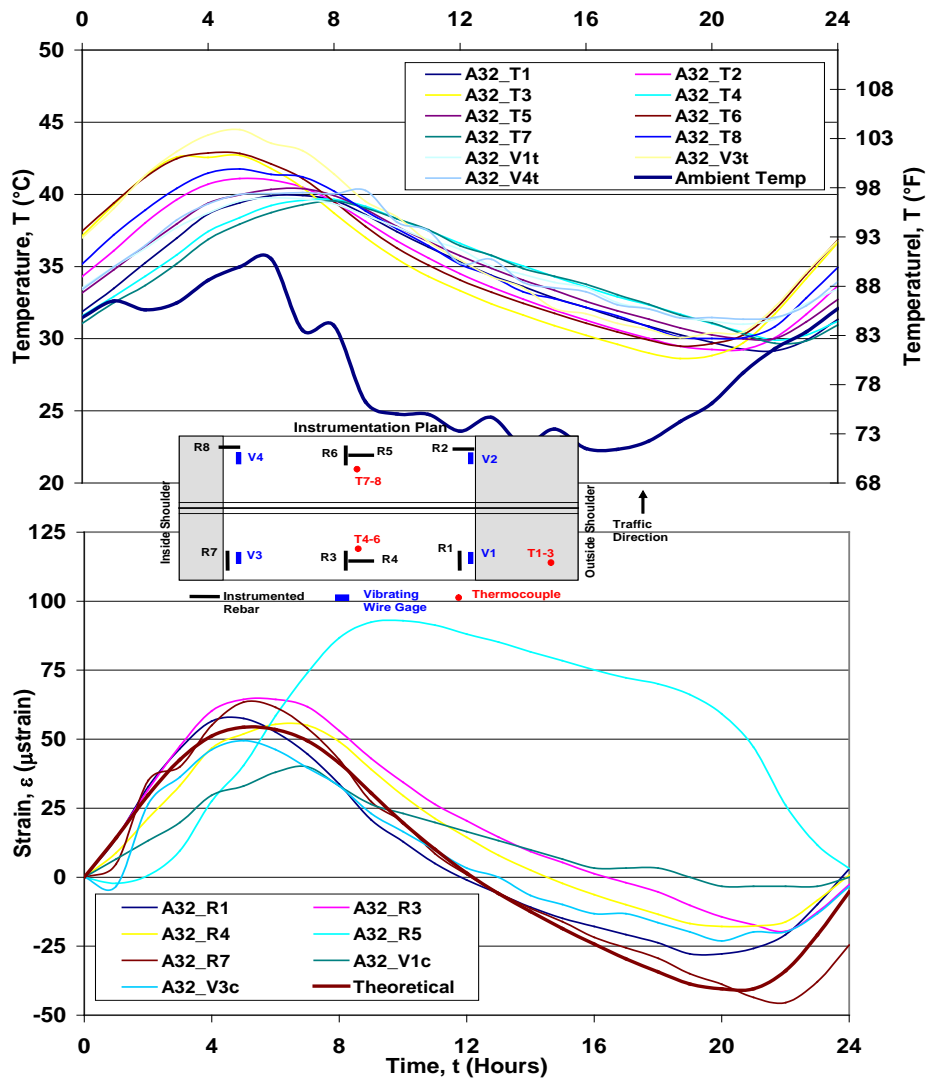


Figure 4.3 – One day window from July 13, 2006 showing all instruments for Panel A32 (a) temperature history (b) strain history

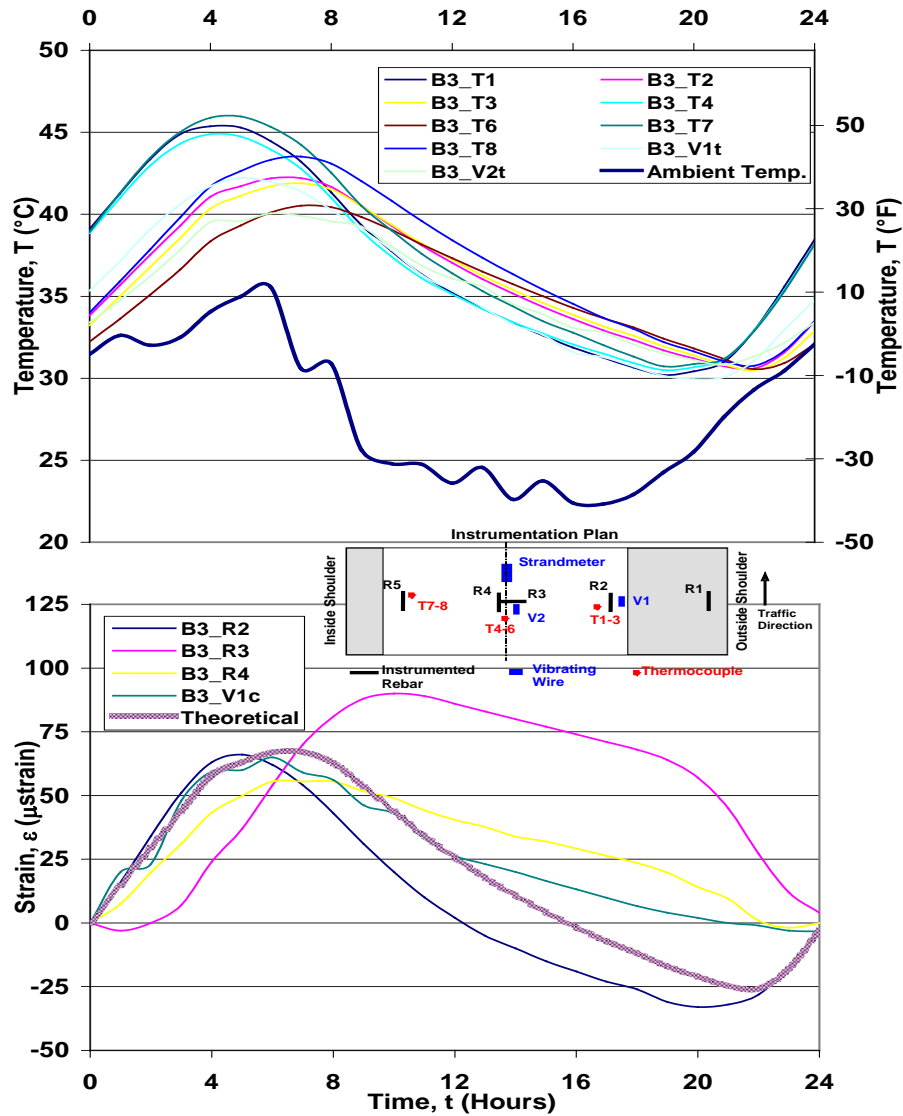


Figure 4.4 – One day window from July 13, 2006 for Panel B3 (a) temperature history (b) strain history

The larger magnitude of temperature excursions and slower rate of recovering in the transverse direction can be attributed to the different levels of restraint provided by the surrounding concrete with respect to the asphalt stabilized base. In the longitudinal direction, the pavement is restrained globally by the adjacent post-tensioned panels. The strain measured in the middle of the panel will be largely dictated by pure thermal

behavior of the concrete sections due to the high level of restraint from the heavy sections adjacent to the panel. Whereas in the transverse direction, the level of restraint from the surrounding concrete with respect to the ground is lower and can take on behavior more indicative of the response from the asphalt concrete base. The CTE of the asphalt concrete base is higher than that of concrete and likely retains its' heat longer than the concrete pavement due to the proximity to the ground and insulation from the pavement.

The difference in magnitudes of the transverse and longitudinal strains can also be attributed in part to “curling” resultant from differential heating/cooling between the top and bottom of the concrete pavement. Curling in the transverse direction is likely to be more than that in the longitudinal direction again due to levels of restraint.

The effect of daily temperature excursions can also be observed by looking at the performance of a typical joint panel during the day. Figure 4.5 (Left) shows the silicone based joint compound receding below the pavement surface during lower temperatures. During the hottest times of the day the joint compound squeezes above the pavement surface and appears to be damaged by vehicles passing over it (Right).



Figure 4.5 – Joint Panel A31 during mild temperatures (Left) and hot temperatures (Right)

4.2.3. Weekly Thermal Behavior

Temperature and strain variations from a medium sized window were analyzed to correlate pavement behavior with extended temperature excursions. Figure 4.6 illustrates the temperature history and associated strain response for a five-day window of a base panel in late September (2006). As expected, with increasing temperatures, the pavement exhibits tensile strains. Cooling produces compressive strains. The responses of the individual rebars are similar to the theoretical values. The temperatures for the theoretical predictions are averaged values between two thermocouples closest to the instrumented rebars. The magnitude of strain recorded by Rebar 2 (thickness of pavement = 8.2 inches) are larger than that of Rebar 4 (thickness of pavement = 11 inches), in part due to Rebar 2 being located in a thinner cross-section of concrete. The concrete strain behavior mimics what is to be expected for a moderate heating trend for the entire duration. The day-to-day localized strain behavior is predictable with having temperature histories.

The rate at which the temperature in the pavement increased or decreased was observed to largely be a function of the proximity of the specific location to an exposed surface and location-specific thickness of the pavement, as seen in Figure 4.6a. Thermocouples 1 and 4 (T1 & T4) had a faster rate of heating and cooling since they were located approximately 2 inches from the top surface of the pavement. It is for this reason that they measured the hottest and most cool temperatures from day to day. The rest of the thermocouples were located at mid-depth or at the bottom 1/3 of the cross-section. As the location of the temperature measurement gets closer to the crown and deeper in the pavement, smaller magnitudes of changes in temperature were observed as

shown in Figure 4.6a. The convention used was as follows: T1 closest to the top surface, T2 in the middle, T3 at the bottom, T4 at top, T5 close to bottom. The exact locations and thicknesses of the pavement at specific instrument locations are presented in Appendix B. Concrete strain, as denoted by the individual devices (R2, R4) is largely proportional to the magnitude of temperature at that cross-section of pavement.

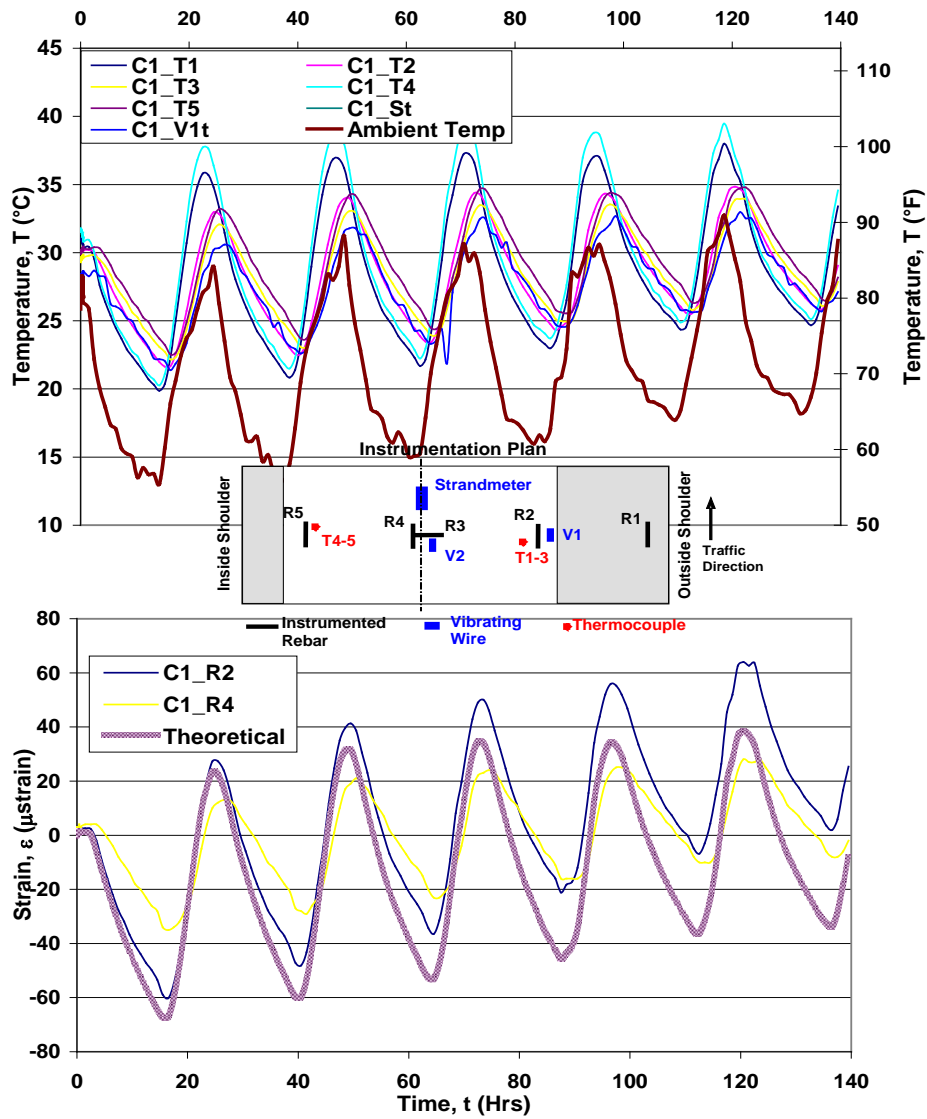


Figure 4.6 – Measured concrete strains in pavement at a short-termed window (a) temperature history (b) strain history

Analysis of results using time windows of different lengths facilitated study of seasonal variations and associated performance of the pavement section. Figure 4.7a shows a moderate heating trend in mid July, including the movement of a cooling front on Day 11 where the mean temperature drops approximately 5°C (9°F). It is readily apparent in Figure 4.7a that the pavement temperatures are higher than the ambient air temperature. The temperature in the pavement stays well above the low temperature at night due to the ground retaining much of its heat. This effect is clearly noted on Day 11 in Figure 4.7 due to the cold front moving and the lowest temperature in the pavement was still above the hottest air temperature of the previous day. Much larger strains were measured by the instrumented rebars compared to the theoretical values, which were validated by comparing with the strain response from the vibrating wire instruments. This is in part due to the only location that temperature was measured in the panel was located near the thickest portion, where the change in temperature is the lowest throughout the day. It was from this temperature measurement the theoretical response was predicted. Larger temperature variations are prevalent in the thinner sections which resulted in larger changes in strain over the individual days. This relationship is indicated in Figure 4.8.

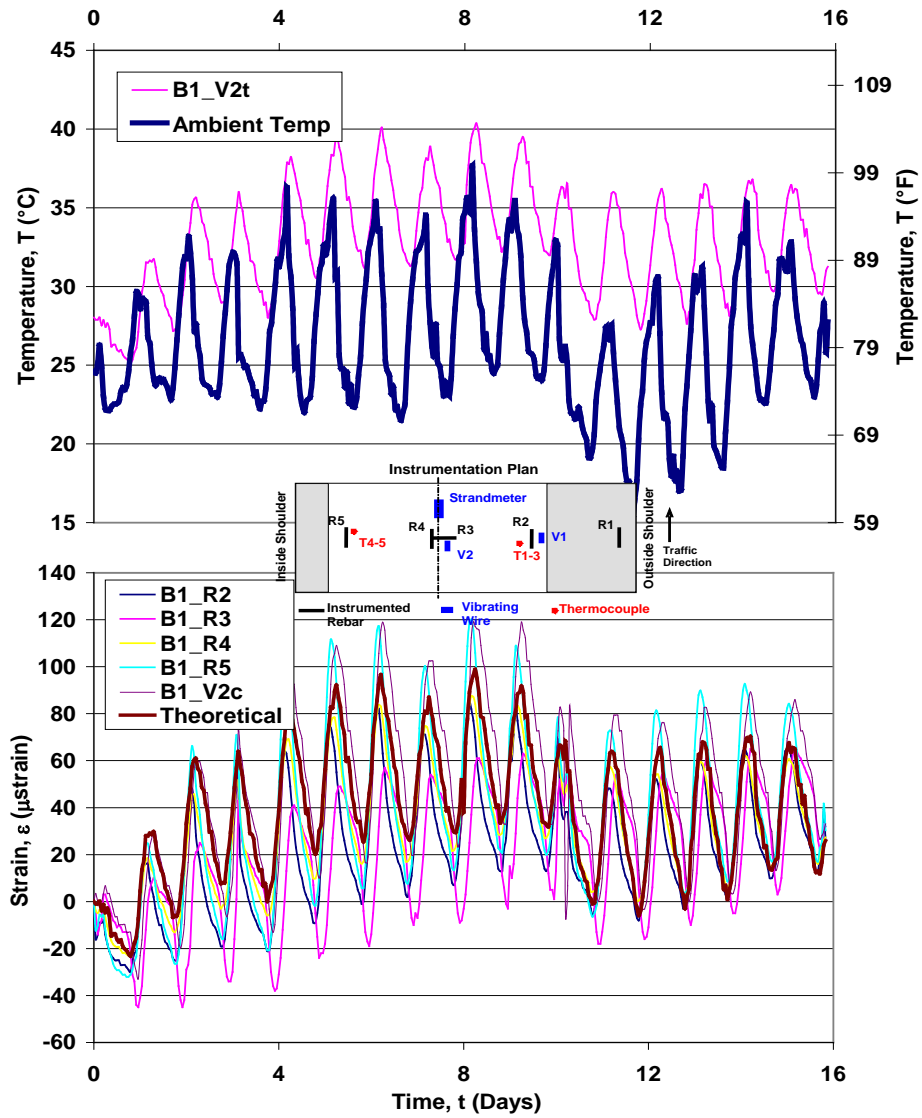


Figure 4.7 – Medium window indicating weekly heating and drastic cold front with associated concrete strains (a) temperature history (b) strain history

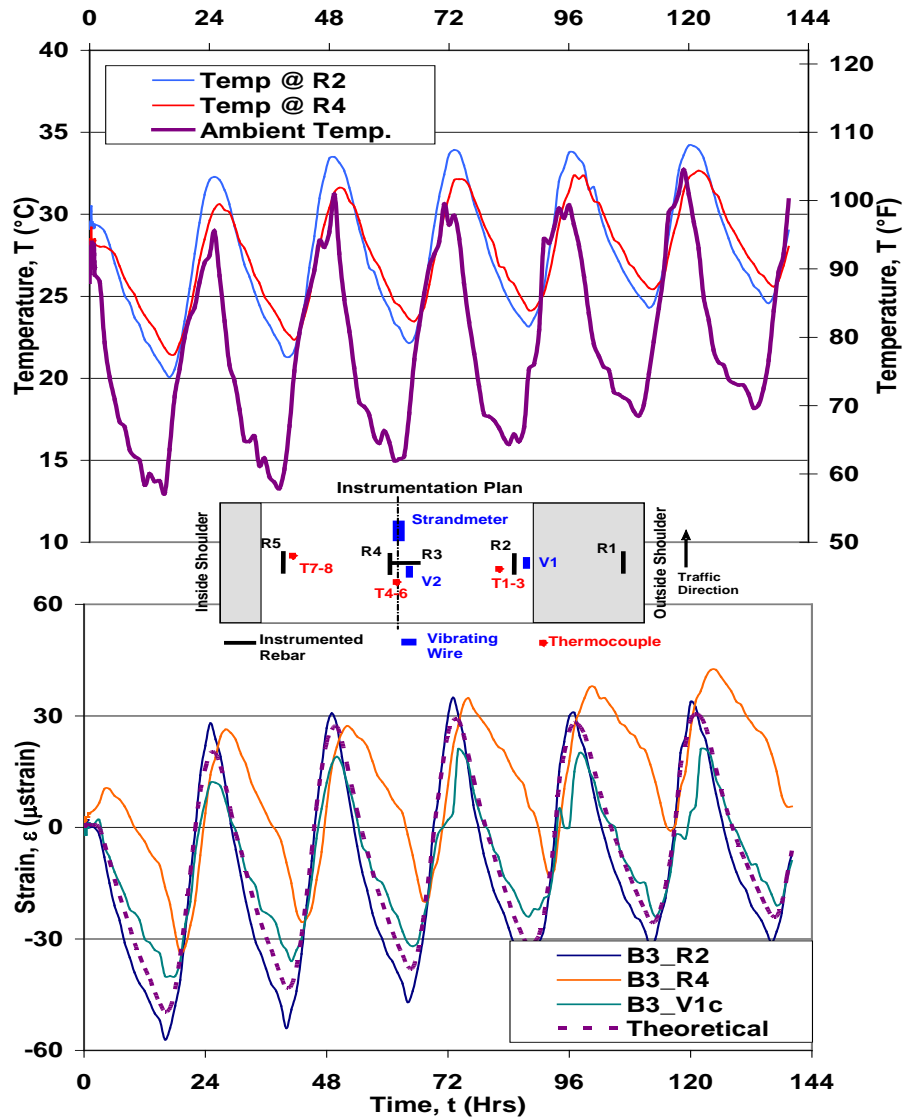


Figure 4.8 – Weekly instrument history for Panel B3 (a) temperature history (b) strain history

4.2.4. Seasonal Variations in Panel and Global Pavement Responses

Analyses were performed to understand the effect of seasonal variations in addition to the earlier discussed daily and weekly temperature fluctuations. By filtering out hourly variations in temperature and strain it was possible to highlight long term and seasonal warming/cooling trends. This was accomplished by comparing mean daily

temperature and strain values (average of 24 hourly data points during each day for each transducer). Figure 4.9 shows a six month window from early October of 2006 to the end of April, 2007. This window of time represents the longest duration without significant interruptions in the data acquisition system. Other windows of time show comparable trends, even if there were frequent weather-related or equipment-related outages and changes in the data acquisition programs to monitor different sets of instrumentation. The plots in the following figures highlight typical winter cooling (October through February) and typical spring heating (February through April) trends and associated strain histories. There are no data for a small period in late November, when the data acquisition system was down due to a power outage. The temperature history in Figure 4.9a includes both mean daily ambient temperature as well as mean daily pavement temperature for Panel B2. It can be observed that the excursion of mean pavement temperature is smaller than that observed for the ambient temperature reflecting the time delay in heating and cooling the concrete pavement and sub-grade mass. As in earlier discussions, it should be noted that the strain plot provides incremental strain history during the time window of interest and does not represent actual strain magnitude (which is less important to the discussions here).

In Figure 4.9 an overall compressive trend (reducing strain magnitude) can be observed as the mean daily temperature drops during winter and similarly a tensile trend (reduced compression) can be observed when the mean temperatures rise during spring. The theoretical concrete strain ($\alpha\Delta T$) is calculated assuming a CTE of $6 \mu\text{strain}/^\circ\text{C}$ (using the average change in temperature recorded by all thermocouples in the panel).

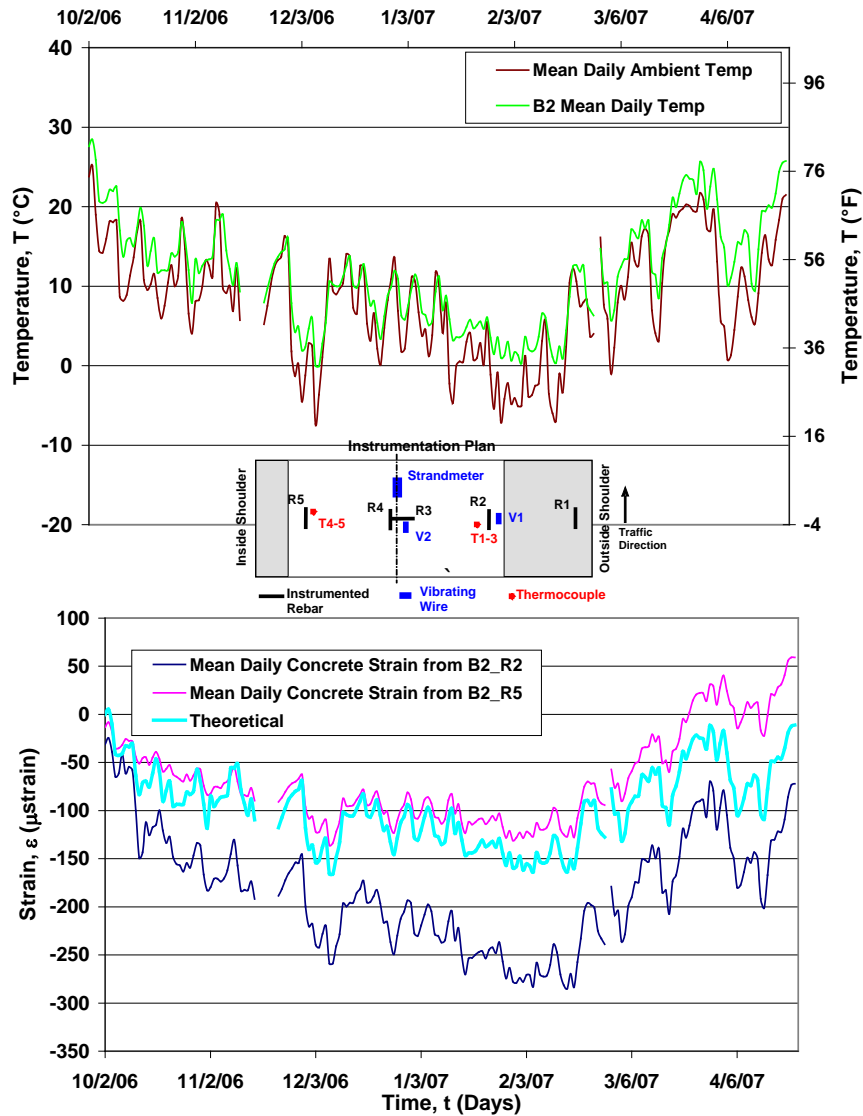


Figure 4.9 – Six month window showing longitudinal concrete strains in Panel B2 at different locations (R2 and R5) (a) temperature histories (b) strain histories

Rebars 2 and 5 (see panel inset in Figure 4.9 for rebar locations) both exhibit expected trends in strain histories given the thermal loading history. Both of these instrumented rebars are located where the pavement thickness is comparable (8.5 inches), and are located at similar heights (4 inches from the bottom). However the magnitudes of

strains at the two locations are significantly different for the same mean daily temperature drop of approximately 26°C (peak strain differential of approximately 140 μ strain for Rebar 5 as opposed to 280 μ strain for Rebar R2 from October 2006 to February 2007). Local sub-grade friction and panel-specific in-plane bending effect due to use of steel wedges along the outer shoulders (and resultant non-uniform panel to panel contact) are likely reasons for variations in strain magnitudes between locations R2 and R5.

While simplistic and idealized this prediction captures the essence of trends in strains from thermal loads. However magnitudes of strains are predicted inadequately. It should be noted that in addition to thermal loads, the strain histories in plots like that shown in Figure 4.9 are also influenced, in a location specific manner, by several other factors including: elastic (modulus) and thermal (CTE) mismatch between pavement and sub-grade and resultant sub-grade friction, restraint due to an improperly performing joint, local thermal variations (differential thermal gradients due to differences in local exposure/dissipation conditions and due to different pavement thicknesses) and changes in prestressing force due to thermal effects. Relatively negligible influences can also be attributed to creep and shrinkage of concrete, relaxation of prestressing steel, traffic loads and strain gradients from bending. Figure 4.10 shows longitudinal strain histories measured from different instrumented panels using instrumented rebars along the passenger side wheel path of the right lane (see inset showing measurement location R2).

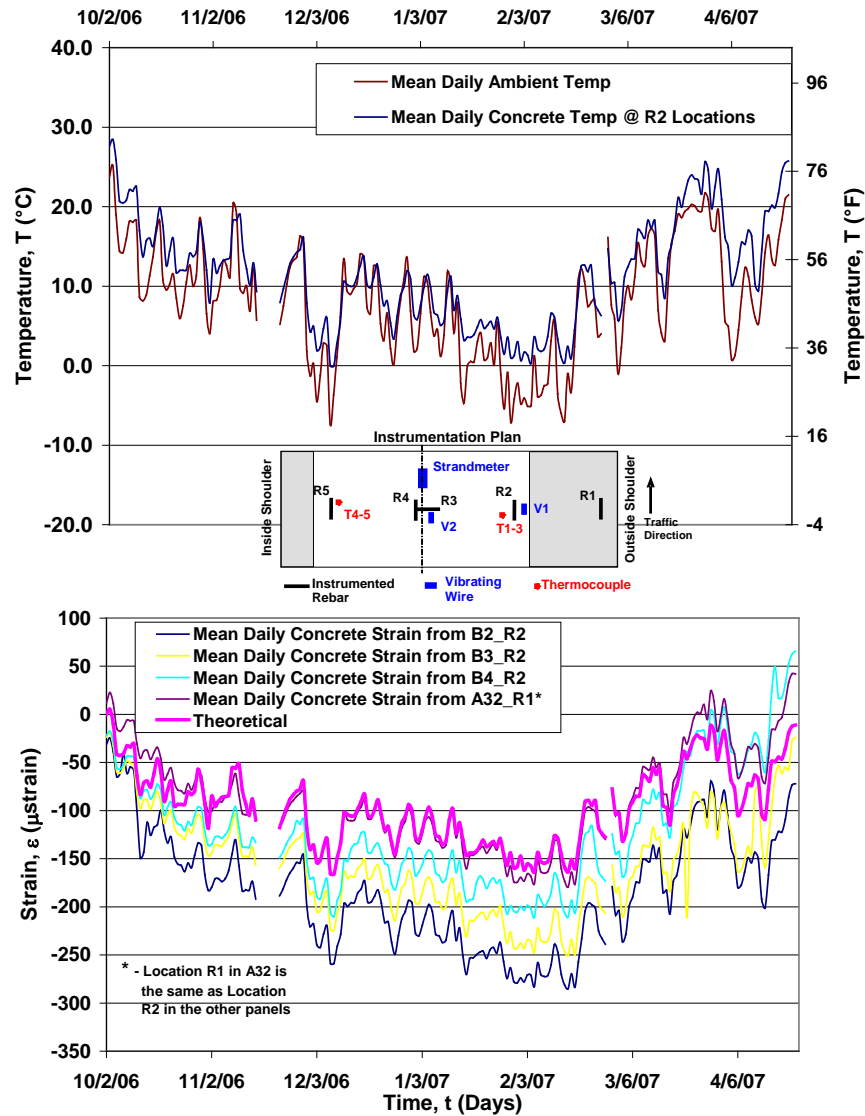


Figure 4.10 – Six month window showing longitudinal concrete strains at identical panel location (R2) in different instrumented panels (a) temperature histories (b) strain histories

It should be noted that location R1 in joint panel A32 is identical to location R2 in all base panels (B2, B3, and B4). It is interesting to observe that strain magnitudes monitored in Figure 4.10b progressively decrease from panel B2 to B3 to B4 and to A32 (from the base panels in the middle of the test section to the joint panel at the end of the test section). While not conclusive, the consistent and progressive reduction of peak

strain magnitudes (around February 2007) suggests that sub-grade friction may have some influence on this behavior. It is also important to observe from this figure, that when temperature returns back to the initial value after approximately 6 months, the differences in strain magnitudes in the various panels do not vanish, suggesting the effect that causes peak strains in these panels to be different is not elastic (friction is an inelastic phenomenon, unlike small thermal expansion/contraction due to seasonal temperature excursions).

Figure 4.11 shows transverse strains measured from different instrumented panels using instrumented rebars near the crown (see inset showing measurement location R3). It should be noted that locations R4 and R5 in joint panel A32 are identical in the transverse plane to location R3 in the base panel. The transverse strain histories across the joint in the joint panel (R4 versus R5) are very similar. The magnitudes (150 – 250 μ strain) of peak strain events for transverse direction are comparable to those in the longitudinal direction (Figure 4.9 and Figure 4.10). Again the magnitudes of compressive strains during the coldest portion of the year are slightly larger than predicted by only thermal behavior suggesting an accompanying change in prestressing force or external frictional characteristic takes place during seasonal variations. The difference in strain magnitude is largest during the middle of winter (February) and decreases as the mean temperatures rise during early spring (April) back to levels similar to those recorded in fall (October). However inconclusive, this strain recovery is more elastic than recorded in the longitudinal direction suggesting it may be due to changing prestress levels and eccentric bending effects caused by uneven stress distributions rather than sub-grade friction.

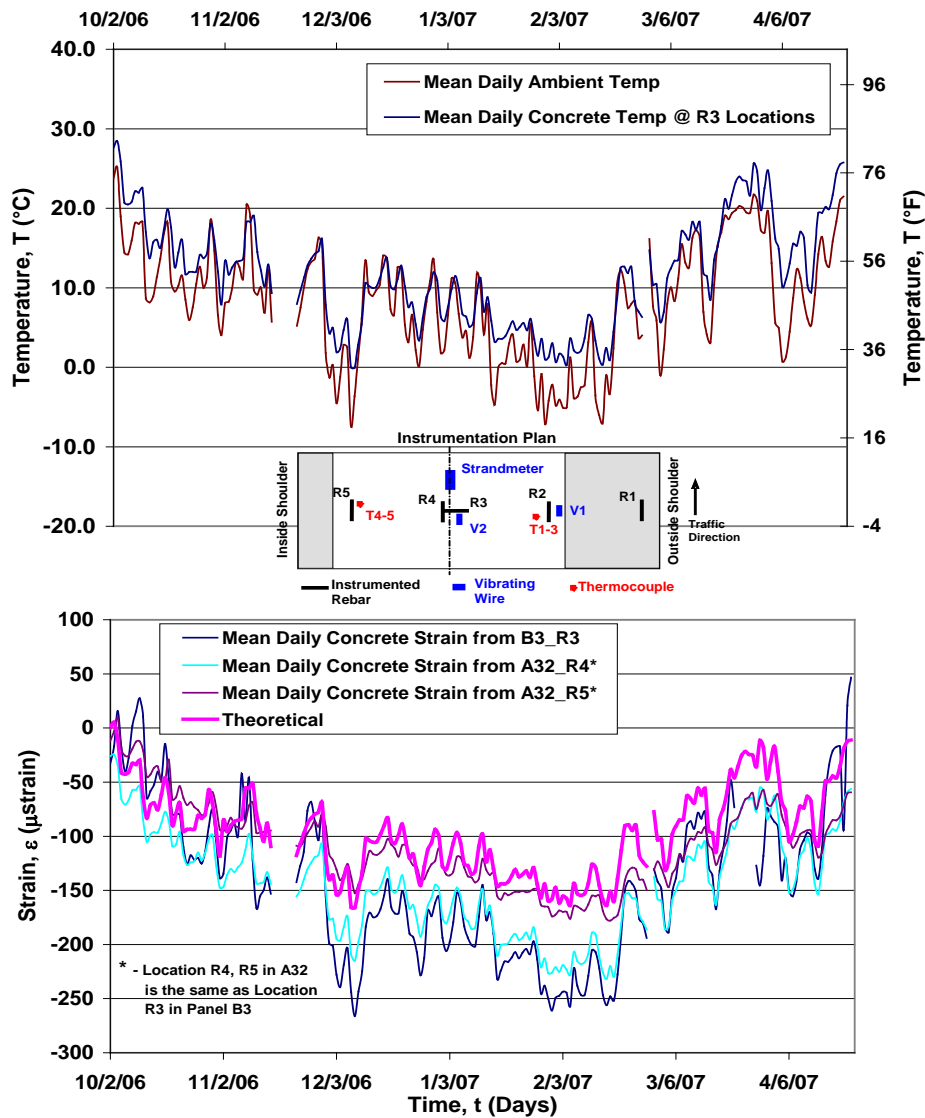


Figure 4.11 – Six month window showing transverse concrete strains at identical panel location (R3) in different instrumented panels (a) temperature histories (b) strain histories

Even while there was initial speculation that long-term drift in strain readings from instrumented rebars might significantly affect strain histories, it is clear from Figure 4.12 that this is not the case. Strain history from instrumented rebar at location R1 in the joint panel A32 is compared with similar history from the vibrating wire gage at the same

location for a two month window during December 2006 – February 2007. The strain histories are nearly identical.

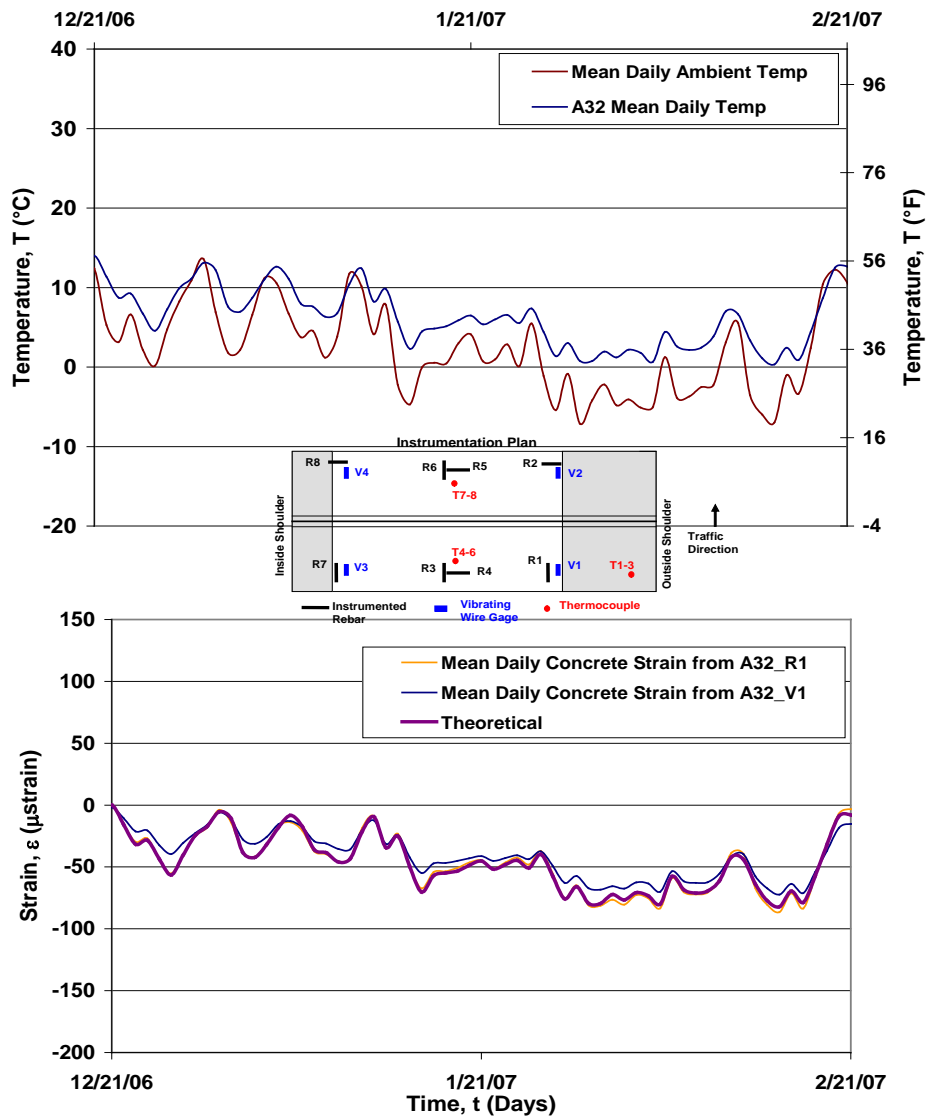


Figure 4.12 – Two month window showing longitudinal concrete strains at identical panel location (R1-V1) measured using instrumented rebar R1 and vibrating wire gage (V1) (a) temperature history (b) strain history

The effect of service temperatures on prestressing force is also of interest from a performance point of view. Figure 4.13 includes a plot of temperature (ambient and pavement temperature at crown at mid-height where the post-tensioning strandmeter monitored is located) and associated strandmeter strain history recorded in Panel C1. If the post-tensioning strand was un-bonded, one would expect strand strain to decrease with a decrease in pavement temperature due to elastic shortening of the pavement section. However, since the post-tensioned strands are grouted, they behave as if they were bonded, with a decrease in temperature producing tensile strains in the strand instead (Figure 4.13b, due to prestressing steel which has a higher CTE being restrained by concrete with a lower CTE – thus producing compression in concrete and tension in steel for the incremental temperature event). Notice that Figure 4.13b shows actual strandmeter strain magnitudes (i.e. uses the actual zero strain reference from the start of the post-tensioning operations, rather than a dummy “zero strain reference” to highlight effect of the temperature event alone). The loss in prestress force from when the post-tensioning operations were completed includes losses due to initial elastic shortening, friction, creep, shrinkage and relaxation. These losses were quantified in Brent Davis’s companion thesis.

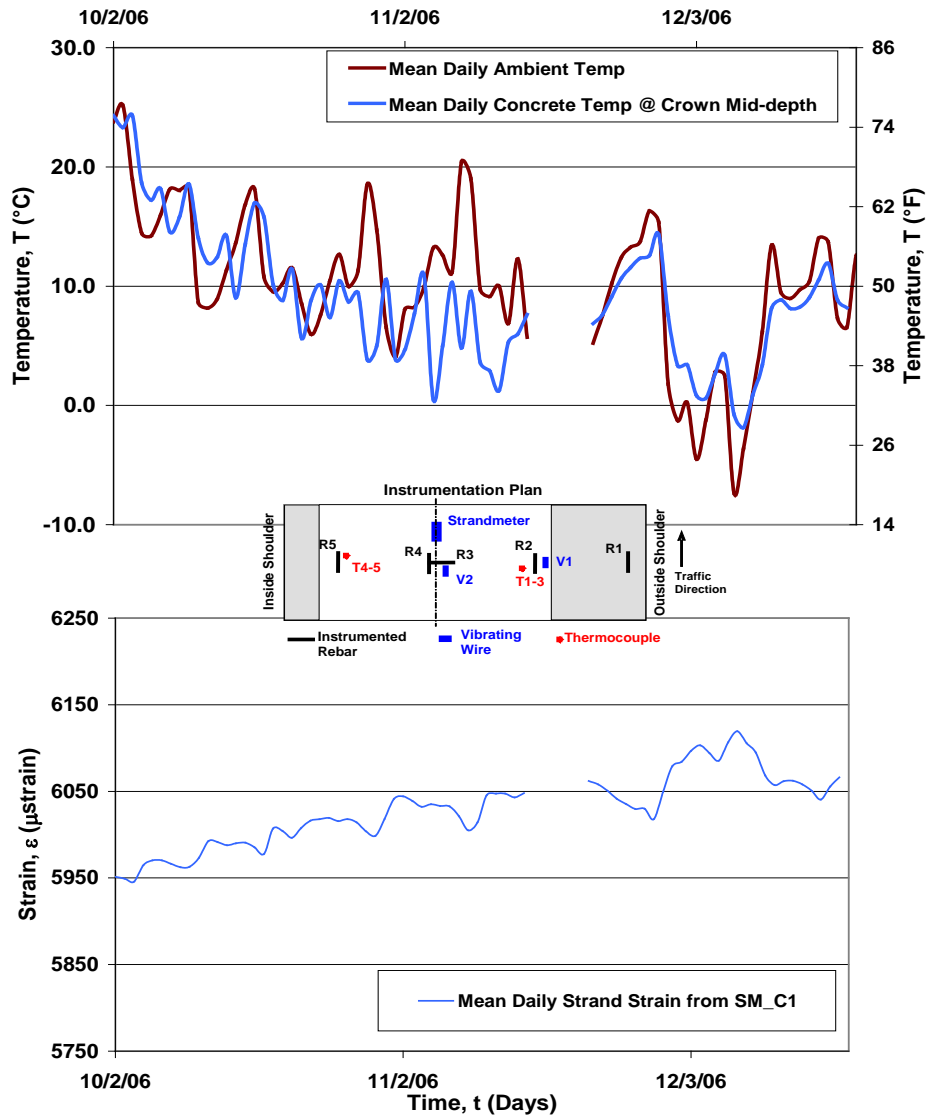


Figure 4.13 – Strandmeter response at center of 250’ test section during typical winter-time temperature excursion (a) temperature histories (b) strain histories

4.3. Pavement Response due to Vehicular Loading

A data acquisition program was designed to isolate vehicular traffic strain from other long-term influences such as temperature, creep, shrinkage and restraint effects. Data was acquired at significantly higher acquisition rates (12 Hz per channel). This

gives a least count of 0.08 seconds since a large amount of data is acquired in a short time, the total acquisition window was reduced to approximately 30 minutes. Simultaneous to automated acquisition of data from the instrumented rebars, visual observation of the traffic history was also recorded so that correlations could be made of strain peaks in the response. An unrelated lane closure (right, outside lane) facilitated visual monitoring of traffic. Traffic speeds were limited to 55 mph as a result of this lane closure. The rebar strain response due to traffic loads on the driver-side wheel path of the inside, left lane is illustrated in Figure 4.14. Since this experiment was performed in the afternoon, the overall compressive trend (negative slope in the global response) seen in Figure 4.14 is a result of the heating of the pavement.



Figure 4.14 - Traffic strain (rebar response) in the pavement at crown

Passenger vehicles were undetectable with respect to the +/- 0.35 μstrain level of noise within the signal of the instrumented rebars. Figure 4.15 displays the concrete response at the crown of the pavement for a selected duration at which visual vehicle

count was also undertaken. Strains induced by tractor trailers on the pavement, which make up approximately 1/3 of the vehicles on I-57, can be seen in Figure 4.15.

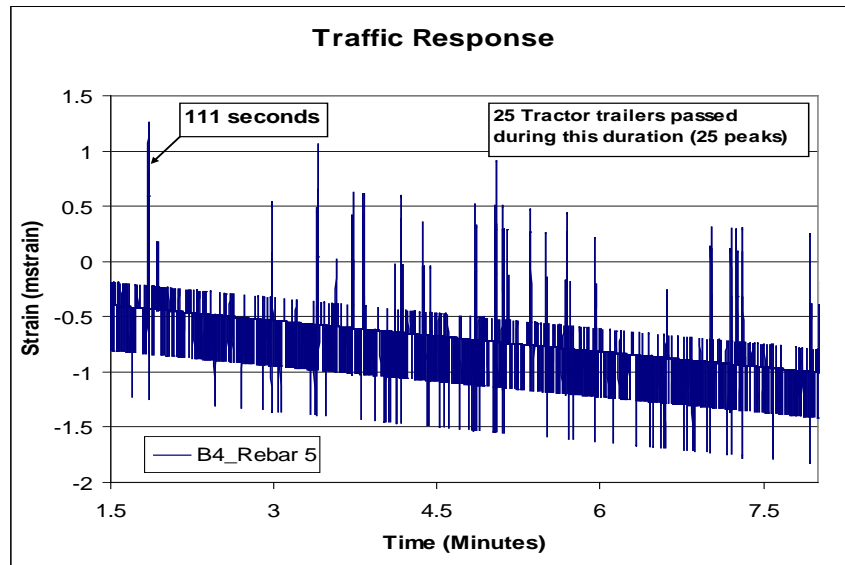


Figure 4.15 – Duration of traffic response that was verified visually

Figure 4.16 illustrates the individual tractor trailer response on the pavement at the crown. The tractor trailer that passed the precast panel being recorded had four axles; one at the front of the tractor, two at the back of the tractor, and one at the rear of the trailer. The three compressive peaks at 111 seconds suggest a correlation to the individual axles passing over the instrumented rebar. The two, rear tractor axles were likely encompassed in the second compressive peak due to their proximity to each other. The tensile peaks are the result of stress caused by the approaching axles that are not quite directly over the instrumented rebar. It is useful to note that strain magnitudes from truck traffic are typically under $\pm 3 \mu\text{strain}$, compared to strains of $\pm 6 \mu\text{strain}$ for a $\pm 1 \text{ }^\circ\text{C}$ excursion in pavement temperature. It is important to note that these strain readings were taken near the neutral axis of the prestressed panels. Assuming a linear gradient, surface

strains (extreme fiber) caused by traffic loading are likely less than 25 μ strain which is a small portion of the total daily strain behavior characterized largely by thermal expansion/contraction.

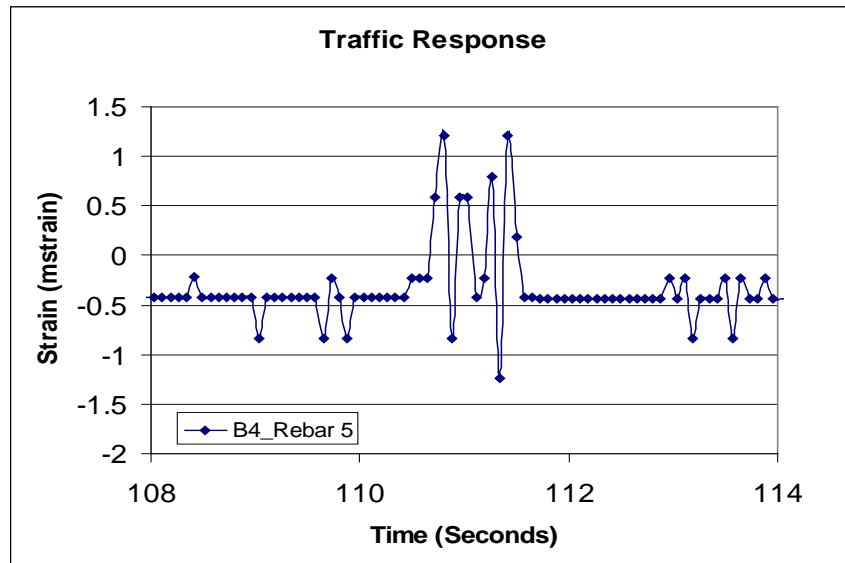


Figure 4.16 – Resulting concrete response from a tractor trailer passing over

4.4. Effective Post-tensioning Stress Distributions

4.4.1. Post-tensioning Stress Distributions Affected by Poor Transfer at Joints

Prestressing provides additional bending resistance in critical areas for service loadings, confinement and crack control. Post-tensioning also locks the panels together globally, helping with load transfer and increasing the stiffness of the pavement sections. This section describes the level of post-tensioning stresses and distribution as indicated by the embedded instrumented rebars. Figures of strain distributions across the width of the panels will aid in investigation of poor prestress transfer.

Comparisons throughout the section can be readily made between the various panels because Rebar 1, 2, 4, and 5 are in the same cross-sectional locations for Panels

C1, B1, B2, and B3. The predictions are shown with expected steps from each pair of strands that are stressed. These steps are also visible in most of the measured data.

Figure 4.17 illustrates concrete behavior of a typical base panel near the center of the 250 ft test section during post-tensioning. The theoretical response predicted was used to compare with the average concrete strain and not the individual rebar responses, whose magnitude is affected by the thickness of the panel at the measurement. By comparing local strain magnitudes at the four locations along the width of the panel, an idealized sense of where force is transferred can be developed. Lowest strains were measured at Rebar 2, then slightly higher at Rebar 4, with the largest stress transfer taking place at the inner and outside shoulders. The poor prestress distribution of this interior panel is likely resultant of several factors that occurred during fabrication and construction as follows.

1. Wooden and Steel shims were used during construction along the outside shoulder (near R1) to correct global alignment problems.
2. The epoxy used to lubricate the edges during the placement and seal off the joint was allowed to harden prior to post-tensioning.
3. During construction, feeding the post-tensioning strands was difficult because the PT ducts were thought to have sagged during fabrication. Due to localized frictional effects, the concrete prestress force near those sections would be affected.
4. Alignment of the post-tensioning ducts may have been difficult to obtain due to no transverse “keyway” or other physical system to align the panels.

Overall post-tensioning levels are obtainable, as represented by the average concrete strain vs. the theoretical strain behavior in Figure 4.17, which was derived from a simple mechanics approach. However, the durability and susceptibility of cracks

opening in localized concrete regions with lower than desired prestressing may come into question in the future. Pre-tensioning will aid in the flexural capacity of these regions and the resistance of surrounding stiffer concrete should minimize any serious susceptibility to crack openings. More often than not for the instrumented base panels near the center of the test section, the post-tensioning strain levels near the R2 location were less than desired, as shown in Figure 4.18. Panel B3 indicates expected prestress levels since it is the closest to the passive jacking end and does not incur the effects of cumulative prestress loss along the length due to the aforementioned problems and also frictional losses, which are discussed in the following section.

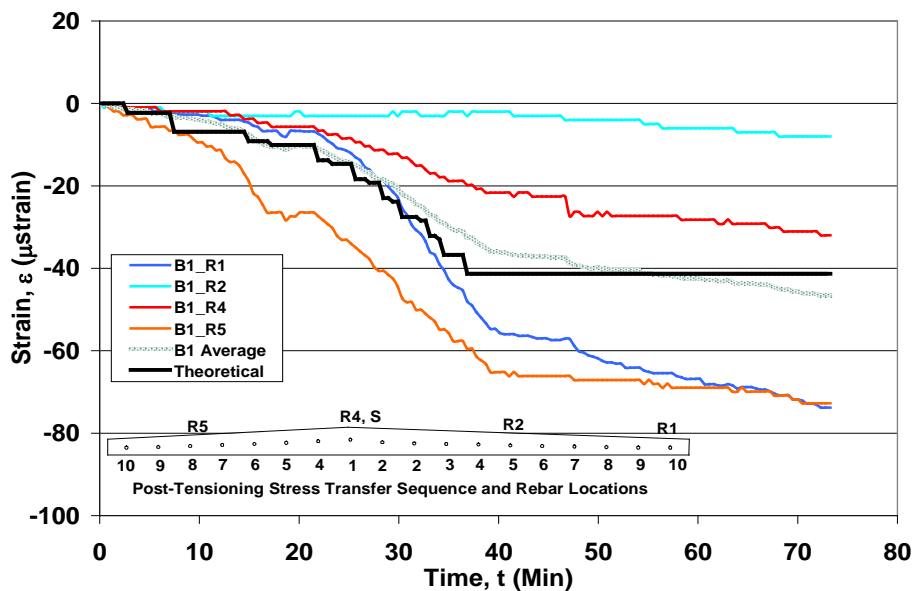


Figure 4.17 – Concrete strain for a typical base panel during post-tensioning operations

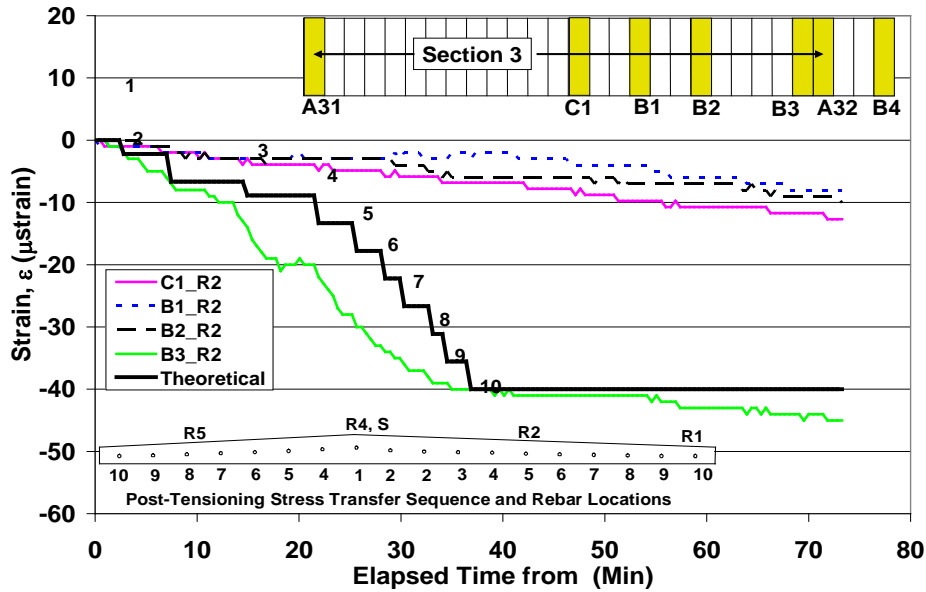


Figure 4.18 – Concrete strain measured at the R2 location (beginning of outside shoulder)

4.4.2. Post-tensioning Stress Losses due to Friction

Measured levels of post-tensioning strains were also affected by several frictional phenomena. It is difficult to extract trends that could be allocated to each type of characteristic loss, but an overall behavior is understood. Levels of post-tensioning stresses transferred to the panels are inhibited by sub-grade friction and friction within the post-tensioning ducts. This is where alignment and possible sagging of the post-tensioning ducts become critical to the effectiveness of prestressing.

Figure 4.19 illustrates the average concrete strain response of the four measurements in each panel for the five panels measured in Section 3 during post-tensioning. There does not exist a nice trend that coincides with frictional losses, primarily because of localized frictional characteristics with the sub-grade (partial regions that were filled with sand where the crane had left ruts provide different resistance than

the asphalt base), localized stress distribution inhibitors such as the shims that were placed between the panels, and the result of only having taken a small sample (four) measurements in each panel. Most importantly Figure 4.19 reinforces that post-tensioning forces are possible to obtain with the implemented design save for working out a few of the minor kinks in the construction and fabrication. Other frictional prestress loss analyses were performed in (Davis 2006).

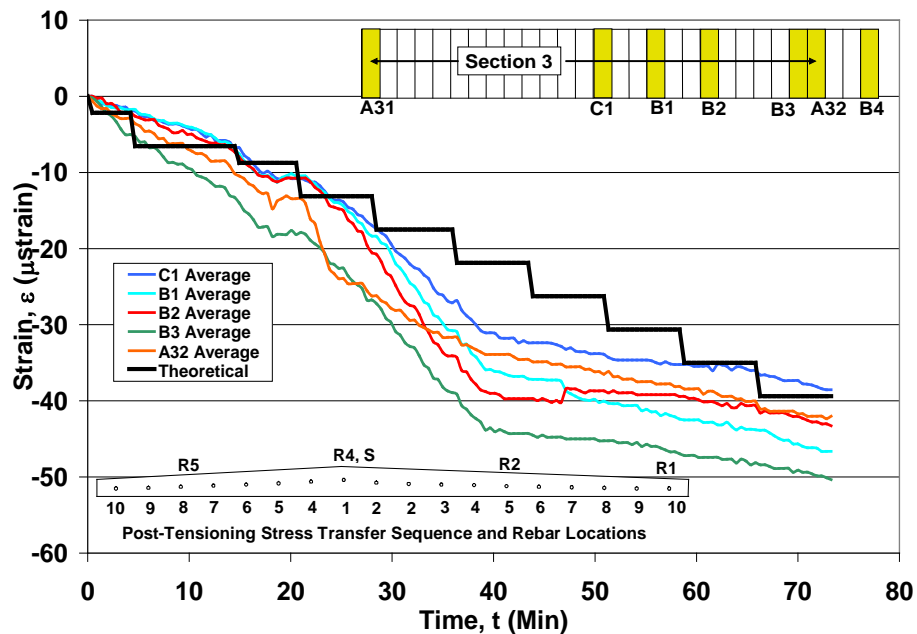


Figure 4.19 – Average Post-tensioning concrete strain histories for instrumented panels

4.5. Transverse and Longitudinal Cracking

Cracking and visual degradation surveys were performed during inspections in the latter half of the 18-month service monitoring. Both longitudinal and transverse cracks have developed in the precast panels. Figure 4.20 and Figure 4.21 show a longitudinal

crack that originated at a corner of a strandmeter block-out. The crack spans several panels suggesting possible influence from external loading such as traffic loads and sub-grade movements. The crack has likely propagated since that lane receives the load from the drivers side wheels of the majority of vehicles and has followed the post-tensioning duct where a reduced cross-sectional area exists. Figure 4.20 (right) shows the outline of the crack that traverses several base panels.



Path of the longitudinal crack

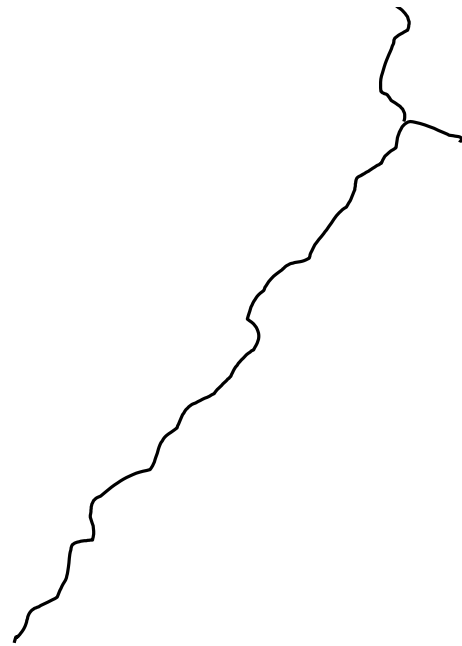


Figure 4.20 - Longitudinal crack in driver side wheel lane

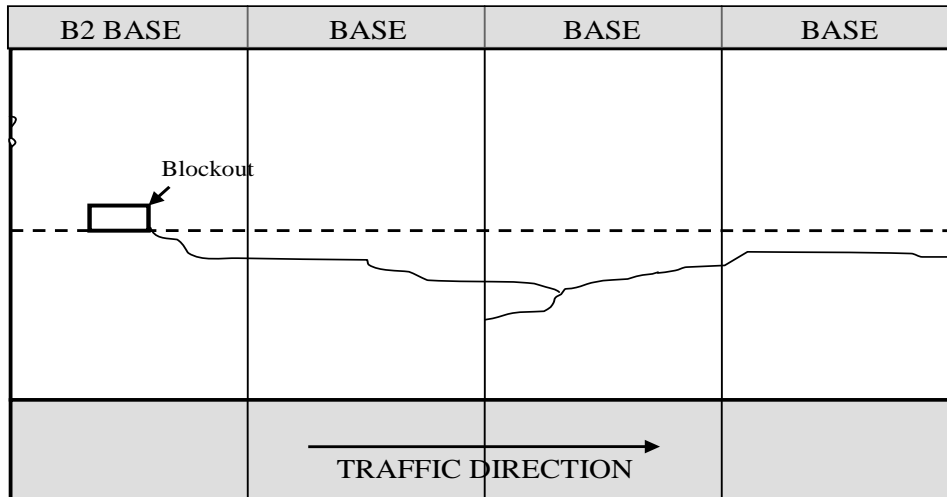


Figure 4.21 - Schematic of one longitudinal crack

Longitudinal cracking have also been documented along the shoulders of the precast panels. Some transverse cracks are located on an observed schematic in Figure 4.22. Longitudinal cracking along the shoulders may also be exaggerated by shims used between panels to correct alignment during construction and limited by perimeter rebars designed for edge reinforcement. Transverse cracking has primarily occurred at the mid-section of the panels. The scaling noted in Figure 4.22 is located on the inside shoulder where the pavement was not ground smooth. An official crack survey has been conducted at several times of the study by MoDOT to locate, measure the length, and record the width of the cracks. It was found that the majority of the cracks are “hair line” cracks.

The difficult issues with PPCP are in the actual implementation of the sophisticated designs. Designs using small post-tensioning ducts are used and may sound appealing for designers, but the manipulation and placement of large, heavy concrete panels that are relatively thin becomes complicated when tight tolerances are required. The higher initial costs associated with PPCP will be offset somewhat by reduced costs due to more rapid construction and potentially reduced maintenance. In any case, it is likely that PPCP may be initially reserved for high volume urban areas where lane closures are both expensive to end users and dangerous for workers and travelers.

Members of the ETG spent time discussing the potential causes of cracking found in the pavement described in the previous section. Some of the more important causes for the cracking observed in the pavement system were identified as;

- Thermal shock due to fabrication of the panels during the winter time in an outdoor bed where panels were steam cured and subsequently exposed to sub-freezing temperatures. Even while only some cracks were visible in the panel prior to placement in the field, it is speculated that residual tensile stresses may have reduced intended levels of prestress.
- The varying thickness of the panel resulted in local non-uniform stresses from prestressing, thermal and restraint loads.
- The effects of epoxy applied between panels that cured well before post-tensioning operations could be completed results in unintended effects.
- Grouting operations used a much larger amount of grout than anticipated. Since no grout was observed exiting the pavement, much of it could have

gone underneath the panels causing upward pressures and uneven stress distributions to the base.

4.5.2. Visual Crack Surveys

The pavement sections were visually inspected each time the research team visited the site. A total of 8 visits were undertaken during the 18-month service performance monitoring of the pavement to inspect the pavement, survey joint performance and troubleshoot instrumentation following weather-related damage to the electronic circuitry. The overall performance of the pavement system has been very good. Two aspects that could use more attention in future projects include “as constructed” joint performance and ways to mitigate pavement-cracking. Both of these issues have not, and are not likely to pose performance problems in the future. However, experience from this project can serve to facilitate design, fabrication and construction improvements where these aspects can be better addressed.

4.6. Joint Panel Performance

The joint panels were designed to open at the pre-engineered construction joint at the center of the panel during post-tensioning operations. However due to difficulties in threading the post-tensioning strands and resulting delays, the contractor decided to place all panels in all four 250 ft sections prior to post-tensioning. This may have affected performance at the joint panels as the original plan was to post-tension one 250 ft section before placing panels for the adjacent section. In addition, the cold joint in the two-step casting of the joint panels had better bonding than anticipated across the joint. As a result

the joint panel between sections 3 and 4 (the more heavily instrumented joint panel – A32) did not open up as designed. However, all other joint panels have performed well during this study. In the contractor’s effort to open the A32 joint using jacks, the concrete fractured adjacent to the intended joint. A patch mix was used to repair the loose concrete and later filled as intended with joint compound. The damaged joint operated fine until the summer of its first year in service. It can be seen in Figure 4.23 that by mid-June with temperatures reaching new highs, the joint compound had started to chip away due to the restrained joint operation. The following photographs (Figure 4.23 – Figure 4.25) illustrate problems with the joint compound in Panel A32. Initially, when the joint compound was squeezed out of the joint it was expected that the joint may deteriorate significantly in time and may exhibit poor performance. However, since the joint compound chipped away due to normal traffic wear, the recorded concrete strain in the panel were similar to that of the base panels located in the middle of the 250 ft section. The joint appeared to be performing well in the most recent inspection in May 2007.



Figure 4.23 – Flexible joint compound squeezing out on a hot day with minor amount of chipping of rigid compound, Joint Panel A32 (June 27, 2006)



Figure 4.24 – Rigid joint compound chipped away more extensively, Joint Panel A32 (August 16, 2006)



Figure 4.25 – Moderate degradation to rigid joint compound, Joint Panel A32 (May 9, 2007)

This page intentionally left blank.

5. Conclusions

5.1. Project Observations

The 1,010 ft precast prestressed pavement system on I-57 in south-eastern Missouri is performing well since being opened to traffic in January, 2006. The pavement surface and prestressed system are in good condition aside from some visible cracking. These cracks, which are present in the transverse and longitudinal directions, are not expected to present problems with regard to the durability or long-term performance of the pavement system. Possible reasons for the cracking observed under service conditions have been detailed in Section 4.5.1

The pilot project was successful and has provided useful insights into improving fabrication and construction techniques that will benefit future projects. The structural design of the panels and their economical implementation will only improve with the experience gained in this and other similar projects.

The following sections outline the summary conclusions based on the evaluation of results from the instrumentation program, companion laboratory tests, observations from construction, and visual inspections of the performance of the precast prestressed pavement system.

5.2. Construction Challenges

The first two challenges are interrelated and stem from the decision by the contractor to lay all 101 panels before installing and post-tensioning strands in each of the 250 feet sections.

- Threading of the post-tensioning strands through the ducts for the 250 feet long sections proved difficult. Suspected impediments to strand installation were cumulative variations in panel-to-panel alignment, misaligned ducts, and possible ice buildup in some of the ducts.
- The usage of epoxy between precast panels to facilitate proper alignment of panel edges hardened due to construction delays with threading the post-tensioning strands. The hardened epoxy bonded the panels together and resulted in the sections behaving as a monolithic 250 ft. unit prior to stressing instead of 25 10-ft. panels. In hindsight, it would have been beneficial to require sequential post-tensioning of the four 250 ft. pavement sections as originally planned.
- Wooden and steel wedges (shims) were inserted between panels along the outer shoulder edge of pavement to correct the global pavement misalignment during placement. The use of these wedges affected the stress distribution during post-tensioning operations as documented earlier in Chapter 4. Use of wedges (particularly stiff high-modulus steel wedges) in such a post-tensioned pavement system should be disallowed for this reason.

5.3. Service Performance

- It has been demonstrated that with appropriate data acquisition sampling rates, monitoring of related embedded instrumentation, and methods of analysis, it was possible to isolate and measure strains from traffic loads, post-tensioning operations as well as thermal loads from daily, weekly, and seasonal trends.
- Pavement strains due to temperature change are significantly larger than all other types of loading (viscous effects such as creep, shrinkage and relaxation, or vehicular loads). Daily longitudinal strains excursions ranging from 50-100 μ strain were observed for cool or mild days. Hot summer days appear to produce strain excursions ranging from 125-200 μ strain.
- Larger magnitude of strain in the transverse direction than the longitudinal direction, while inconclusive, indicates lower levels of restraint transversely.
- Additionally, thermal gradients were observed due to varying pavement thicknesses and exposure conditions (top versus bottom pavement surface).
- Measured vehicular loadings produced approximately 1-2 μ strain in the precast pavement at the location of measured strain. This constitutes only 1-2% of the total strain produced from daily thermal loading.

5.4. Pavement Longevity

The future performance of the precast prestressed pavement system is expected to be without significant problems. The precast prestressed technology that has been adapted for use as a pavement system has been proof-tested in previous decades of bridge projects. However it would be naïve to say that among the multitude of pavement problems that exist, none will arise. It is certain that many of the known significant challenges, addressed earlier, have been targeted in the design of the prestressed pavement system which will enable it to perform as well as or better than its traditional pavement counterparts. The areas that are expected to meet or exceed design expectations are the following:

- Ability of the pavement system to span voids that may form in the base material due to erosion or settlement.
- Due to the built in compressive stresses in the prestressed pavement, cracks are expected to stay closed. The smaller crack widths compared to a non prestressed pavement are likely to minimize damage due to water intrusion and resultant freeze-thaw.
- Increased material durability due to improved quality control at a precasting yard.

5.5. Recommendations for Future Work

Future crack surveys should be performed to develop an understanding of the extent of crack growth. If the extent of cracking is increasing, then potential causes could be predicted with higher certainty by studying the problematic areas. Although the

cracking currently present does not appear to have been or become detrimental to the pavement system, it was not a desirable outcome. Further inspection and sampling on a multi-seasonal level could provide useful data indicating the severity of the cracking and possible extent of moisture intrusion. Useful information on the expected performance can allow preventative measures to be performed to minimize detriments.

In-situ chloride permeability tests should also be performed after the pavement has been subjected to deicing salts to determine the rate of chloride ingress in the field. These results can then be compared to baseline readings taken on virgin specimens and compared to field results of other pavement types. This testing may provide useful knowledge on material specific performance unique to the pavement system.

REFERENCES

- ASTM (1998). Standard Practice for Capping Cylindrical Concrete Specimens, ASTM:5.
- ASTM (2002). Standard Test Method for Flexural Strength of Concrete (Using Simple Beam with Third-Point Loading, ASTM: 3.
- ASTM (2002). Standard Test Method for Fundamental Transverse, Longitudinal, and Torsional Resonant Frequencies of Concrete Specimens, ASTM: 7.
- ASTM (2003). Standard Test Method for Resistance of Concrete to Rapid Freezing and Thawing, ASTM: 6.
- ASTM (2005). Standard Test Method for Compressive Strength of Cylindrical Concrete Specimens, ASTM: 7.
- ASTM (2005). Standard Test Method for Electrical Indication of Concrete's Ability to Resist Chloride Ion Penetration, ASTM: 6.
- ACPA (2004). Concrete Types, American Concrete Pavement
- Dailey, C. (2006). Instrumentation and Early Performance of an Innovative Prestressed Precast Pavement System. *Civil and Environmental Engineering*. Columbia, University of Missouri – Columbia.
- Davis, B. M. (2006). Evaluation of Prestress Losses in an Innovative Prestressed Precast Pavement System. *Civil and Environmental Engineering*. Columbia, University of Missouri – Columbia.
- Degussa (2006). Degussa Admixtures. 2006.
- Eatherton, M. (1999). Instrumentation and Monitoring of High Performance Concrete Prestressed Girders. *Civil Engineering*. Columbia, University of Missouri - Columbia.
- Geokon (1996). Instruction Manual Model VCE - 4200, Geokon, Inc.
- Gopalaratnam, V. S., B. M. Davis, et al. (2007). Performance Evaluation of Precast Prestressed Concrete Pavement, RI03-007. Columbia, University of Missouri – Columbia.
- Maxim (2007). iButton Instruction Manual Model DS1922L, Maxim IC, Inc.

- Merritt, D., F. B. McCullough, et al. (2000). The Feasibility of Using Precast Concrete Panels to Expedite Highway Pavement Construction. Austin, TX.
- Merritt, D. K., F. B. McCullough, et al. (2001). Feasibility of Precast Prestressed Concrete Pavements. 7th International Conference on Concrete Pavements.
- Merritt, D. K., B. F. McCullough, et al. (2002). Construction and Preliminary Monitoring of the Georgetown, Texas Precast Prestressed Pavement, Center for Transportation Research; University of Texas at Austin: 140.
- Transtec (2005). Personal Correspondence. Precast Panel Design Drawings.
- Transtec (2009). Precast Pavement. www.precastpavement.com.
- Tyson, S. S. and D. K. Merritt (2005). Pushing the Boundaries, Federal Highway Administration. 2006.

APPENDIX A

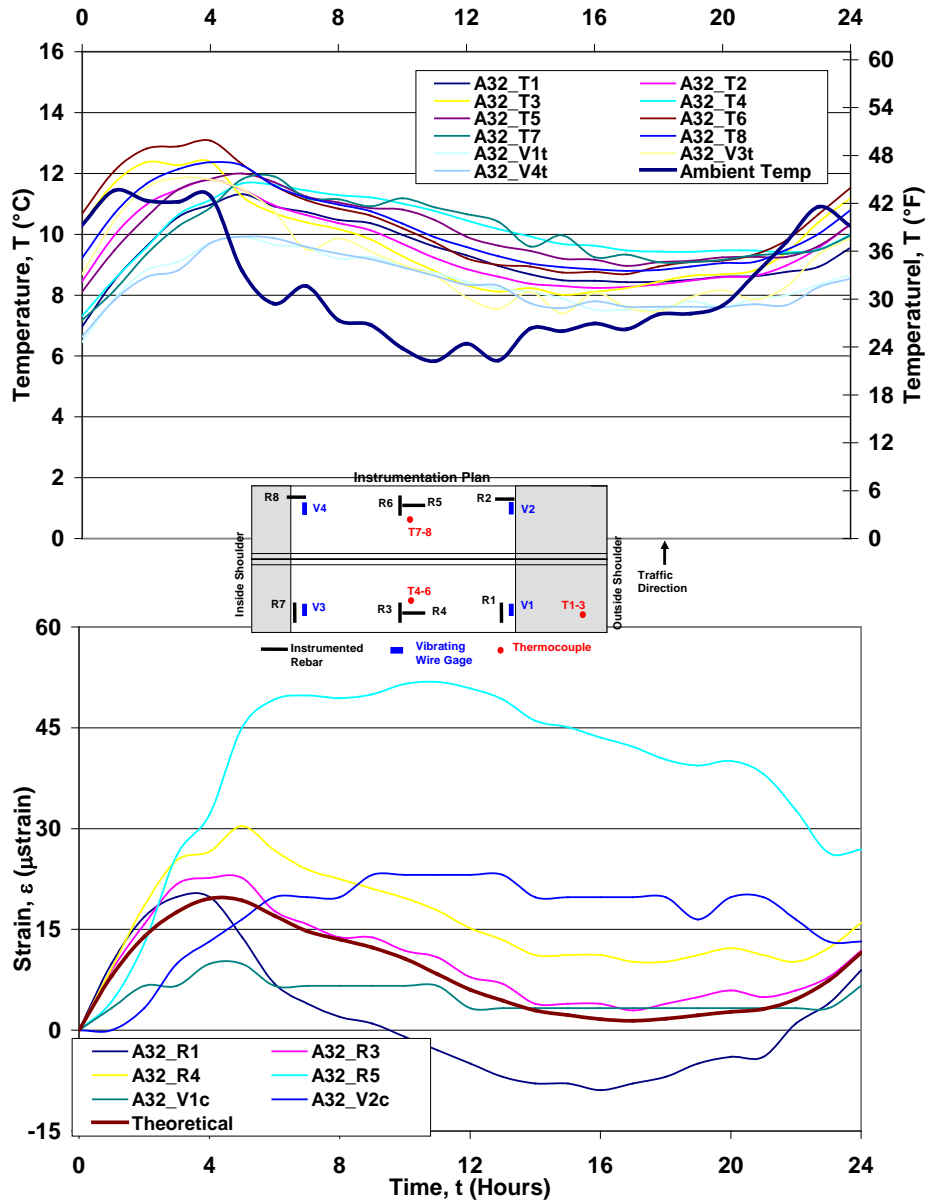


Figure A.1 – One day window from 12/27/2006 for Panel A32 (a) temperature history (b) strain history

APPENDIX B

The exact locations of instruments (rebars, thermocouples, vibrating wire) used in this project are tabulated below.

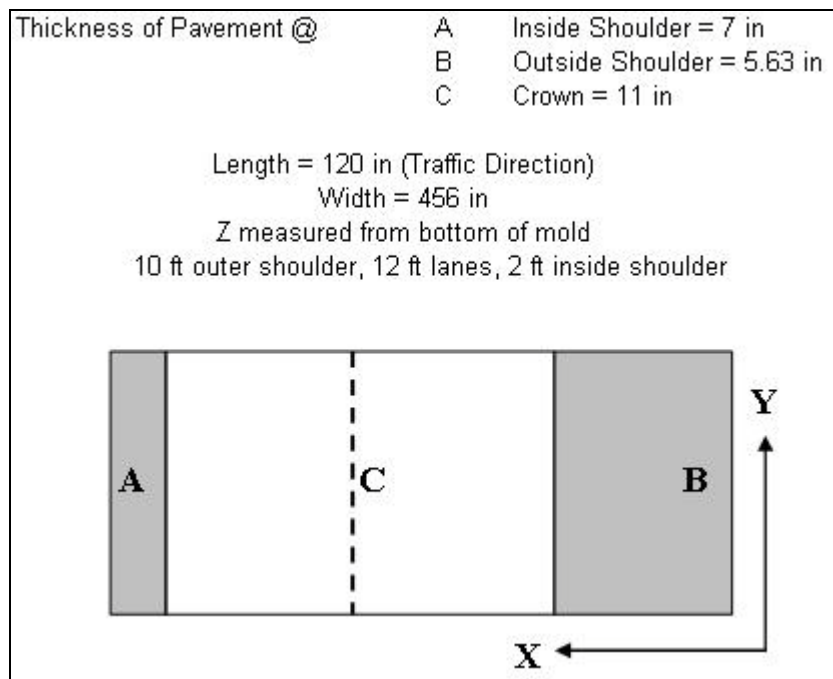


Figure B.1 – Convention for gage locations

| Panel C1 | X (in) | Y (in) | Z (in) | Depth X Section (in) |
|-----------------|-------------------|-------------------|-------------------|---------------------------------|
| R1 | 31 | 45 | 3 | 6.3 |
| R2 | 142 | 48 | 4 | 8.5 |
| R3 | 264 | 52 | 7 | 11.0 |
| R4 | 264 | 44 | 4 | 11.0 |
| R5 | 384 | 62 | 4 | 8.5 |
| T1 | 126 | 70 | 2 | 8.2 |
| T2 | 126 | 70 | 4 | 8.2 |
| T3 | 126 | 70 | 7 | 8.2 |
| T4 | 364 | 52 | 2 | 8.9 |
| T5 | 364 | 52 | 7 | 8.9 |

Table B.1 – Locations of instruments used in Panel C1

| Panel B1 | X (in) | Y (in) | Z (in) | Depth X Section (in) |
|---------------------|-------------------|-------------------|-------------------|---------------------------------|
| R1 | 29 | 60 | 2.5 | 6.2 |
| R2 | 137 | 62 | 4 | 8.4 |
| R3 | 252 | 55 | 4 | 10.8 |
| R4 | 256 | 60 | 4 | 10.8 |
| R5 | 378 | 62 | 4 | 8.6 |
| T1 | 121 | 54 | 1 | 8.1 |
| T2 | 121 | 54 | 3 | 5.6 |
| T3 | 121 | 54 | 6 | 5.6 |
| T4 | 366 | 68 | 3 | 8.9 |
| T5 | 366 | 68 | 7 | 5.6 |
| V1 | 137 | 62 | 4 | 8.4 |
| V2 | 256 | 60 | 4 | 10.8 |

Table B.2 – Locations of instruments used in Panel B1

| Panel B2 | X (in) | Y (in) | Z (in) | Depth X Section (in) |
|---------------------|-------------------|-------------------|-------------------|---------------------------------|
| R1 | 27 | 60 | 4 | 6.2 |
| R2 | 142 | 60 | 4 | 8.5 |
| R3 | 254 | 56 | 4 | 10.8 |
| R4 | 260 | 62 | 4 | 10.9 |
| R5 | 392 | 47 | 4 | 8.3 |
| T1 | 142 | 67 | 1 | 8.5 |
| T2 | 142 | 67 | 3 | 8.5 |
| T3 | 142 | 67 | 7 | 8.5 |
| T4 | 364 | 52 | 1 | 8.9 |
| T5 | 364 | 52 | 6 | 8.9 |
| V1 | 142 | 60 | 4 | 8.5 |
| V2 | 260 | 62 | 4 | 10.9 |

Table B.3 – Locations of instruments used in Panel B2

| Panel B3 | X (in) | Y (in) | Z (in) | Depth X Section (in) |
|---------------------|-------------------|-------------------|-------------------|---------------------------------|
| R1 | 20 | 46 | 3 | 6.0 |
| R2 | 138 | 62 | 4 | 8.4 |
| R3 | 251 | 54 | 2 | 10.7 |
| R4 | 262 | 59 | 4 | 11.0 |
| R5 | 379 | 60 | 4 | 8.6 |
| T1 | 145 | 57 | 2 | 8.6 |
| T2 | 145 | 57 | 4 | 8.6 |
| T3 | 145 | 57 | 6 | 8.6 |
| T4 | 289 | 58 | 3 | 10.5 |
| T5 | 289 | 58 | 6 | 10.5 |
| T6 | 289 | 58 | 8 | 10.5 |
| T7 | 361 | 67 | 2 | 9.0 |
| T8 | 361 | 67 | 4 | 9.0 |
| V1 | 138 | 62 | 4 | 8.4 |
| V2 | 262 | 59 | 4 | 11.0 |

Table B.4 – Locations of instruments used in Panel B3

| Panel B4 | X (in) | Y (in) | Z (in) | Depth X Section (in) |
|---------------------|-------------------|-------------------|-------------------|---------------------------------|
| R1 | 31 | 61 | 3 | 6.3 |
| R2 | 140 | 63 | 4 | 8.5 |
| R3 | 255 | 54 | 2.5 | 10.8 |
| R4 | 264 | 61 | 4 | 11.0 |
| R5 | 375 | 62 | 4 | 8.7 |
| T1 | 145 | 54 | 1 | 8.6 |
| T2 | 145 | 54 | 4 | 8.6 |
| T3 | 145 | 54 | 7 | 8.6 |
| T4 | 355 | 54 | 2 | 9.1 |
| T5 | 355 | 54 | 4 | 9.1 |
| T6 | 355 | 54 | 7 | 9.1 |
| V1 | 140 | 63 | 4 | 8.5 |
| V2 | 264 | 61 | 4 | 11.0 |

Table B.5 – Locations of instruments used in Panel B4